Doctoral Dissertation（Shinshu University）

Development and characterization of nano functionally graded materials

March 2014

WANG YI

Table of Contents

Abstract

In this work, in order to make a further step on developing the nanofiller employed and polymer based functionally graded material (FGM), the exploration of fabricating nano FGM under different condition is conducted, also the properties of FGM is characterized.

(1) Vapor-grown carbon-fiber (VGCF)-incorporated polymer-based functionally graded materials (FGMs) using a centrifugal method were produced. Gradual VGCF incorporation within an epoxy resin effectively produced depth gradients in the fiber distribution, microstructure, mechanical, and electrical conductivities and microwave absorbing properties. This VGCF-grading capability indicated that it is possible to tailor desired gradient filler content distributions by careful selection of the processing parameters to control variations in the property and microstructure precisely. The results confirmed that the volume content of VGCF in the epoxy substrate increased as a function of the normalized thickness along the centrifugal force direction, which caused a gradient. A uniform VGCF gradient in the composite can also be observed using field-emission scanning electron microscopy. In the case of the electrical properties, for example, the volume resistance exhibited a depth-graded distribution in the matrix as the electrical conductivity of the FGM nicely followed the grading direction; this is considered to be ideal for applications demanding an electrically conductive surface and an insulating core for FGMs. The results of microwave absorption behavior of FGMs indicate that the grading structure can lead to a graded absorption ability, which could be a better design for microwave absorption materials. The concept of FGMs bridges conventional materials and

nanocomposites and will be effective for wider material applications.

(2) Functionally graded multiwalled carbon nanotube (MWCNT) reinforced epoxy matrix composites are fabricated using a centrifugal method. Aggregation of the MWCNTs during the epoxy curing process is prevented using a two-step aminosilane modification. Chemical interaction of the silane with the oxidized nanotube surface is confirmed using Fourier transform infrared spectroscopy and X-ray photoelectron spectroscopy. Raman spectroscopy of acid-treated MWCNTs corroborates the formation of surface defects owing to the introduction of carboxyl groups. The mechanical and microwave absorption property gradients of the composites correspond with those produced via silane modification indicating potential application to microwave absorbing materials. The MWCNTs are better dispersed in the epoxy resin after the modification, making it possible for them become efficiently graded in the epoxy matrix. We therefore show that it is possible to fabricate functionally graded nanofiller-reinforced materials using the centrifugal method by modifying the surface of the nanofiller.

(3) Functionally graded nano-TiO_2 epoxy matrix composites were successfully fabricated using a centrifugal method. In the preparation of the composite, the aggregation of nano-TiO_2 occurred during curing, which had a negative effect on the composite performance. To solve this problem, we introduced a silane coupling agent to modify the surface of the nano-TiO_2, thereby improving the performance and mechanical properties simultaneously. The modified nano-TiO_2 (s-TiO_2) had better dispersion in the epoxy resin, making it possible to produce depth gradients of the mechanical properties of functionally graded materials (FGMs). The s-TiO_2 was characterized with respect to functional groups, morphology, and chemical elements

using transmission electron microscopy, X-ray photoelectron spectroscopy, and Fourier-transform infrared spectroscopy. The results show that a silane layer was successfully coated on the surface. Also, the gradients of the mechanical and permittivity properties of the FGM indicated that by modifying the surface of the nano-filler, it is possible to fabricate nano-filler-reinforced epoxy matrix FGMs using a centrifugal method.

(4) The electromagnetic (EM) wave absorption performance of the FGMs and homogeneous material (HM) was compared and discussed. Based on the approximate calculation, FGMs displayed a better absorption property than HM in the whole range of frequency. The graded structure design is suggested to used to fabricate the EM wave absorbing materials.

List of figures

Chapter 1

General Introduction

General Introduction

1.1 Functionally graded materials

The concept of functionally graded materials (FGMs) was proposed in 1984 in order to solve the problem on thermal barrier materials during a space plane project in Japan [1]. Since then, it has attracted great interest worldwide in terms of designing and combining entirely different materials to control the structure and composition in order to obtain materials with continuously changing properties and functions, for use in challenging applications. Based on the decades' effort of research in FGMs area, significant progress was achieved in the aspects of foundational theory, processing technologies, modeling simulation and practical application [2-11].

1.1.1 Development of FGMs

The theoretical papers by Bever and Duwez [12], and Shen and Bever [13] in 1972 have already showed the value of functionally graded composites with graded structure. However, their work had only concerned about impact, which may due to not much processing method for preparing FGMs [14]. After 12 years, the concept of FGMs was introduced in Japan, then systematic research on manufacturing processes for FGMs was carried out in the framework of a national research program on FGMs. At that time, the scientists wanted to solve the crack problem due to thermal stress which happened to the airplane. Because when the airplane returned to earth from the out space, the surface of the airplane have to expose itself into ultrahigh temperature due to ultrahigh speed. In that circumstance, the metal cannot stand high temperature

up to 2000K, thus the high temperature resistant material such as ceramics have to be employed, but simply laminate the two kinds of material will lead to thermal stress which happened in the interface between the materials, and result in crack. In this case, the concept of FGMs was raised, and well solved the problem. As shown in Fig. 1-1, the material properties such as thermal expansion coefficient and thermal conductivity can gradually change from the outside to inside of surface. In that case, the sudden change can be avoided compared with the laminate materials.

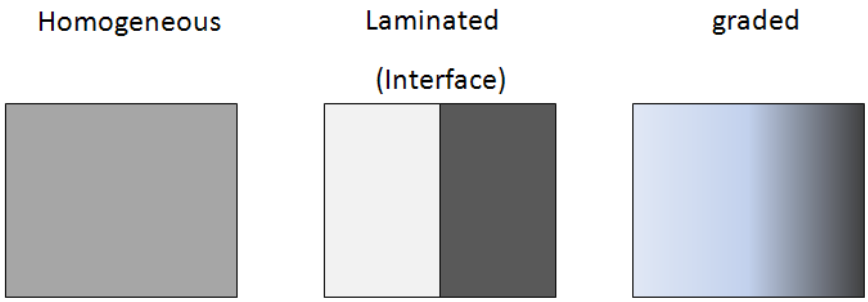

Fig 1-1 schematic showing the difference between FGM and the other material.

From then on, by the variation in composition and structure gradually over volume, resulting in corresponding changes in the properties of the material, which called as FGMs, become very popular, and researchers start to combine entire different materials together for special application.

1.1.2 Processing techniques of FGM and its application

Generally, there are two points that have to be considered when produce a FGM,

that is, how to make a graded structure and then how to let the gradient structure exist in a bulk material. Grading processes can be classified into constitutive, homogenizing and segregating processes. For the constitutive processes, the graded structure of the material or powder is build up in advance. Then in the process of homogenizing, the sharp interface between two kinds of materials is converted into a gradient. After that, by applying an external force such as centrifugation force, the homogeneous structure of materials converted into a graded structure [14-16].

After the continuous graded structure build up, usually drying and sintering or solidification is applied to make a bulk FGM. Based on the basic process concept above, many effective ways to produce a FGM have been developed until now.

1.1.2.1 Powder metallurgy

The powder metallurgy (PM) is one of most viable routes for FGM [17], it is the process of blending fine powdered materials, pressing them into a desired shape or form (compacting), and then heating the compressed material in a controlled atmosphere to bond the material (sintering). The powder metallurgy process generally consists of four basic steps: powder manufacture, powder blending, compacting, and sintering. Compacting is generally performed at room temperature, and the elevated-temperature process of sintering is usually conducted at atmospheric pressure.

Gang et al. developed Mullite/Mo functionally graded material with a powder metallurgy process. They found that the FGM specimens had better thermal shock resistance than did monolithic mullite. And the thermal shock resistance of FGMs was influenced by the sintering-induced residual thermal stress. Also the mechanism

of crack formation was discussed [18].

A functionally-graded biomaterial in a hydroxyapatite (HA)–Ti system was developed by an optimized powder metallurgical process by Chu et al [19]. As a result, HA–Ti FGM is a promising biomaterial for use as a hard-tissue replacement implant, considering its mechanical behaviors.

Zhu et al. fabricated ZrO2–NiCr functionally graded material, and the suitable fabrication procedure of FGM was determined. The results shows that the mechanical properties of ZrO2–NiCr system strongly depend on constitutional variation, and display various graded distributions as well [20].

1.1.2.2 Melt processing

In contrast to PM, the materials first processed under molten state, by applying the external field, the gradient structure can be achieved effectively, and the bulk FGMs can be obtained after subsequent consolidation. In this kind processing, the centrifugal casting and sedimentation casting are considered quite effective and convenient way to fabricating FGMs [21-30].

Watanabe et al. have studied the motion of ceramic particles in a molten metal of a viscous liquid under a centrifugal force, and it is numerically modeled to study the formation process of composition gradients. The simulated results are in good agreement with those of experiments that used a plaster-corundum model FGM. For the centrifugal casting, the process parameter is very important, with modeling results, the gradient structure can be controlled much more precisely [31].

Gao et al. conducted a combined experimental and numerical investigation of the solidification process during gravity casting of FGMs. The interplay between

solidification and particle transport was elucidated in relation to creation of gradient structures in FGMs. The multiphase solidification model developed in this study was extensively validated against the experimental results and generally good agreement was found. Simulations for the Al/SiC FGMs indicated that by optimizing the processing conditions, such as particle size, initial particle concentration, cooling rate and superheat, one can engineer a desired gradient in the solidified part [32].

1.1.2.3 Other methods

Various methods such as chemical vapor deposition (CVD), physical vapor deposition (PVD), plasma spraying are used in inhomogeneous functional graded technology to control the constituent elements of a composite material [33-37]. The vapor deposition method can be used to fabricate a film or a platelike material directly without melting or sintering. Furthermore, composition control of dispersion is comparatively easy in the direction perpendicular to the deposition surface. For instance, Thick ceramic films in the systems TiO_2 and Ti-O-Si consisting of nanocrystalline grains between 15 and 45 nm are prepared by a modified CVD method [38], and Ti-TiC and Ti-TiN FGMs have been fabricated using PVD [39].

Kim et al. reported a C/SiC compositionally graded layer were deposited on the C/C composites by a low pressure chemical vapor deposition (LPCVD) method at deposition temperatures of 1100 and 1300 °C. The deposition conditions of the entire compositional range of the C/SiC composites were determined using a thermodynamic calculation [40].

Carbide coatings deposited by PVD techniques was presented by Nobili et al. Nanocomposite coatings with hydrocarbon matrix were deposited after growing a

functionally graded interlayer and their tribological properties were investigated both in air and in water [41].

1.1.2.4 Application of FGMs

From spaceship to biomaterials for medical application, the FGMs have been widespread and applied in many kind of area [42-45].

For example, Watari et al. reported the titanium/hydroxyapatite (Ti/HAP) and other FGM implants with the concentration changed gradually in the longitudinal direction of cylindrical shape were fabricated by powder metallurgy to optimize both mechanical properties and biocompatibilities or change bioreactivity in each region. The results demonstrated that the tissue reaction occurred gradiently in response to the graded structure of FGM, which implies the possibility to control the tissue response through the gradient function of FGM [46].

1.2 Development of Nano-FGMs

For current research, the field of nanotechnology is one of the most popular areas. The property changes as the particle or fiber dimensions decrease to the nanoscale level, and the synergistic advantage of nanoscale dimensions relative to larger scale modification is an important consideration. Nowadays, the nanotechnology have been developed in basically all technical disciplines [47-51].

Preparing FGMs with nano particle is a challenging work. Nano particle has its own problem of aggregation when disperse in the matrix. The dispersion have been always the main obstacle for the nanocomposites in industry application.

However, Watanabe et al. have developed a novel fabrication method, which called

the centrifugal mixed-powder method, by which FGMs can be obtained containing nano-particles. Using this processing method, Cu-based FGMs containing SiC particles and Al-based FGMs containing TiO_2 nano-particles on their surfaces have been fabricated [52].

Estili et al. established a new and cost-effective technology to overcome these obstacles and mass-produce homogeneous, individually dispersed CNT–alumina ceramic matrix composite powders with a broad range of CNT concentrations (0–15 vol.%) required for FGM processing, which can be densely consolidated by spark plasma sintering (SPS) in shorter times and at lower temperatures [53].

1.3 Polymer based FGMs

As the matrix, polymer has unique advantage because of its excellent mechanical and electrical insulation properties, lightness, and low cost. Due to the limitation of processing methods for polymer FGMs, there are not so much application compared to ceramic or metal based FGMs. To fabricate a polymer based FGM, Usually, similar to melt processing, a gradient of the reinforcement should be introduced prior to polymerization.

Chekanov et al. [54] accomplished an ascending frontal polymerization in a body with a moving boundary. This new method gives an excellent opportunity to prepare functionally gradient materials because composition of a monomer feed stream can be varied in a programmable manner. Polymer samples with hyperbolic gradients of optical dye concentration were manufactured at ambient pressure and temperature.

Klingshirn et al.[55-56] reported centrifugal method to produce polymer based FGMs. A relative continuous gradient in the filler concentration could be realized by

controlling the centrifugal parameter such as the rotation speed and time, or adjusting the viscosity of the resin. The hard filler particles or fibers can improve the thermosetting polymers. It was demonstrated that the gradient in filler content leads to a corresponding gradient in micro hardness and wear resistance.

1.4 Outline of the dissertation

The concept of FGM have greatly inspired the passion to design various kinds of material, as described above, FGM have been applied to many different challenging area. Although different kinds of matrix and filler have been tested and characterized until now, the nanofiller employed and polymer based FGM is still not fully developed compared with metal or ceramic based FGM, part of the reason may be due to a lack of suitable processing technology. However, the continually effort on the research of FGM and further profound cognition for FGM will provide a foundation for developing FGMs.

In order to make a further step on developing the nanofiller employed and polymer based FGM, we explored to fabricate nano FGM under different conditions. In this dissertation, the detailed contents are as follows;

Chapter 1 General introduction

A brief summary is presented about the development history of FGMs, various methods applied to fabricate FGM, application of FGM in different area, also introduced nanofiller employed or polymer based FGMs.

Chapter 2 Development of functionally graded VGCF/polymer materials under relative high viscosity environment

VGCF-incorporated polymer-based FGM is produced using the centrifugal method.

The gradual VGCF incorporation within an epoxy resin effectively caused depth gradients in the tribological behavior, electrical conductivity and microwave absorption properties of the FGMs.

Chapter 3 Functionally graded epoxy composites using silane coupling agent functionalized MWCNTs under relative low viscosity environment

The surface of MWCNTs is successfully modified, ands-MWCNT polymer-based FGMs using a centrifugal method are produced. The gradual incorporation of the s-MWCNTs in the epoxy resin resulted in the formation of deep-penetrating gradients in the distribution, mechanical properties, electrical properties, and microwave shielding properties.

Chapter 4 Fabrication of functionally graded nano-TiO_2-reinforced epoxy matrix composites under relative low viscosity environment

The aggregation problem of TiO_2 have been successfully resolved by modification with silane agent, and confirmed by the result of TEM images, XPS investigation and FTIR test. Also s-TiO_2-incorporated polymer-based FGMs using a centrifugal method are produced. The gradual incorporation of s-TiO_2 into the epoxy resin effectively caused depth gradients in the s-TiO_2 distribution, mechanical properties and dielectric property of the composite.

Chapter 5 Theoretical analysis of EMI SE by absorption between FGM and homogeneous material

Based on the discussion above, the FGMs have a better absorption property than homogeneous material (HM) in the whole range of frequency. The graded structure design is suggested to fabricate the electromagnetic (EM) wave absorbing materials.

Chapter 6 General conclusion

General conclusions about developed nanofiller employed and epoxy based FGMs are presented in this chapter.

References

[1] M. Koizumi, Compos. Part. B., 28b (1997) 1.

[2] G. N. Praveen, J. N. Reddy, Int. J. Solids. Struct., 35 (1998)4457.

[3] F. Erdogan, Compos. Eng., 5(1995) 753.

[4] C. T. Loy, K. Y. Lam, J. N. Reddy, Int. J. Mech. Sci., 41 (1999) 309.

[5] A. J. Markworth, K. S. Ramesh, W. P. Parks, J. Mater. Sci., 30 (1995) 2183.

[6] J. Yang, H. S. Shen, Compos. Struct., 54 (2001) 497.

[7] Z. H. Jin, R. C. Batra, J. Mech. Phys. Solids., 44 (1996) 1221.

[8] B. Kieback, A. Neubrand, H. Riedel, Mat. Sci. Eng. A-Struct., 362 (2003) 81.

[9] V. Birman, L. W. Byrd, Appl. Mech. Rev., 60 (2007) 195.

[10] J. Woo, S. A. Meguid, Int. J. Solids. Struct., 38 (2001) 7409.

[11] J. H. Kim, G. H. Paulino, Int. J. Numer. Meth. Eng., 53 (2002) 1903.

[12] M. B. Bever, P. F. Duwez, Mater. Sci. Eng. 10 (1972) 1.

[13] M. Shen, M. B. Bever, J. Mater. Sci. 7 (1972) 741.

[14] B. Kieback, A. Neubrand, H. Riedel, Mater. Sci. Eng., A362 (2003) 81.

[15]K. Takagi, J. F. Li, S. Yokoyama, J. Eur. Ceram. Soc., 23 (2003) 1577.

[16]L. Prchlik, S. Sampath, J. Gutleber, Wear, 249 (2001) 1103.

[17]J. C. Zhu, Z. D. Yin, Z. H. Lai, Zh, J. Mater. Sci., 31 (1996) 5829.

[18]G. Jin, M. Takeuchi, S. Honda, Mater. Chem. Phys., 89 (2005) 238.

[19]C. L. Chu, J. C. Zhu, Z. D. Yin, Zd, Mat. Sci. Eng. A-Struct., 271 (1999) 95.

[20]J. C. Zhu, Z. H. Lai, Z. D. Yin, Zd, Mater. Chem. Phys., 68 (2001) 130.

[21] Y. Watanabe, N. Yamanaka, Y. Fukui, Z. Metallkd.88 (1997) 717.

[22] Y. Watanabe, H. Eryu, K. Matsuura, Acta Mater. 49 (2001) 775.

[23] G. Zimmermann, A. Schievenbusch, In: W.A. Kaysser (Ed.), Functionally

Graded Materials 1998, Proceedings Of The 5th International Symposium On Fgm 1998, Trans Tech Publications, Switzerland, (1999) 533.

[24] Y. Watanabe, H. Eryu, K. Matsuura, Acta. Mater., 49 (2001) 775.

[25] Y. Watanabe, N. Yamanaka, Y. Fukui, Metall. Mater. Trans. A., 30 (1999) 3253.

[26] Y. Watanabe, A. Kawamoto, K. Matsuda, Compos Sci Techno., 62 (2002) 881.

[27] J. W. Gao, C. Y. Wang, Mat. Sci. Eng. A-Struct., 292 (2000) 207.

[28] P. M. Biesheuvel, V. Breedveld, A. P. Higler, Chem. Eng.Sci., 56 (2001) 3517.

[29] P. M. Biesheuvel, H. Verweij, J. Am. Ceram. Soc., 83 (2000) 743.

[30] Y. Watanabe, T. Nakamura, Intermetallics, 9 (2001) 33.

[31] Y. Watanabe, N. Yamanaka, Y. Fukui, Compos. Part. A-Appl. S.,29 (1998) 595.

[32] J. W. Gao, C. Y. Wang, J. Heat. Trans-T. Asme.123 (2001) 368.

[33] M. Sasaki, T. Hirai, Nippon Seramikkusu Kyokai Gakujutsu Ronbunshi-Journal Of The Ceramic Society Of Japan, 99 (1991) 1002.

[34] A. H. Wu, W. B. Cao, C. C. Ge, Mater. Chem. Phys. 91 (2005) 545.

[35]Y. G. Jung, S. W. Park, S. C. Choi, Mater. Lett.,30 (1997) 339.

[36]M. Sasaki, T. Hirai, J. Eur. Ceram. Soc., 14 (1994) 257.

[37]C. C. Ge, A. H. Wu, Y. H. Ling, Yh; High-Performance Ceramics 2001, Proceedings Book Series: Key Engineering Materials, 224-2 (2002) 459.

[38] S. Seifried, M. Winterer, H. Hahn, Scripta. Mater., 44 (2001) 2165.

[39] T. Hirai, M. Sasaki, Jsme Inter. J. Series I-Solid. Mechan. Stren. Mater., 34 (1991) 123.

[40] J. I. Kim, W. J. Kim, D. J. Choi, Carbon, 43 (2005) 1749.

[41] L. Nobili, F. Pagano, P. L. Cavallotti, Int. J. Surf. Sci. Eng., 2 (2008) 350.

[42]S. Liao, W. Wang, M. Uo, Biomater, 26 (2005) 7564.

[43]E. Muller, C. Drasar, J. Schilz, Mat. Sci. Eng. A-Struct., 362 (2003) 17.

[44]F. Erdogan, B. H. Wu, J. Therm. Stresses., 19 (1996) 237.

[45]B. L. Wang, Y. W. Mai, X. H. Zhang, Acta Mater, 52 (2004) 4961.

[46] F. Watari, A. Yokoyama, M. Omori, Compos. Sci. Technol., 64 (2004) 893.

[47]P. T. Hammond, Advan. Mater., 16 (2004) 1271.

[48]D. R. Paul, L. M. Robeson, Polymer, 49 (2008) 3187.

[49]W. Bauhofer, J. Z. Kovacs, Compos. Sci. Technol., 69 (2009) 1486.

[50] P. Sharma, S. Ganti, N. Bhate, Appl. Phys. Lett., 82 (2003) 535.

[51]B. Wetzel, F. Haupert, M. Q. Zhang, Compos. Sci. Technol., 63 (2003) 2055.

[52] Y. Watanabe, H. Sato, E. Miura-Fuijwara, Materials, 2 (2009) 2510.

[53] M. Estili, K.Takagi,A. Kawasaki,Scripta. Mater., 59, 703 (2008).

[54] Y. A. Chekanov, J. A. Pojman, J. Appl. Polym. Sci., 78 (2000) 2398.

[55] C. Klingshirn, M. Koizumi, F. Haupert, H. Giertzsch, K. Friedrich, J. Mater. Sci. Lett., 19 (2000) 263.

[56] C. Klingshirn, M. Krumova, F. Haupert, K. Friedrich, Composites Sci. Technol., 61 (2001) 557.

Chapter 2

Development of Functionally Graded VGCF/Polymer Materials under Relative High Viscosity Environment

Development of Functionally Graded VGCF/Polymer Materials under Relative High Viscosity Environment

2.1 Introduction

Since the concept of functionally graded materials (FGMs) was proposed in Japan in 1984, it has attracted great interest worldwide in terms of designing and combining entirely different materials to control the structure and composition in order to obtain materials with continuously changing properties and functions, for use in challenging applications [1]. Polymer-based FGMs, which are an important type of FGM, have been developed rapidly because of their low cost and lightness [2–4]. Many achievements have been made in recent years. SiC particles and carbon fiber shave been used as reinforcing agents in polymer matrixes; based on these experiments, simulations of polymer-based FGMs have been developed [5, 6]. However, in order to develop advanced FGMs with excellent properties and multifunctions, the introduction of grading agents is necessary. Vapor-growth carbon-fibers (VGCFs), nanosized fillers, have high aspect ratios, so VGCFs have the advantages of low percolation thresholds and high interface areas. Also, because of the electrical conductivity of VGCFs, nanocomposites based on low concentrations of such fillers may possess novel combinations of electrical, optical, and mechanical properties [7, 8].

However, to date, there has been little research on the fabrication or modeling of polymer-based FGMs incorporating VGCFs. The nanoscale of VGCFs can cause problems because they are difficult to disperse and have poor interface compatibility.

For this reason, it leads to the lack of appropriate processing technology for synthesizing composites containing VGCFs from a homogenous to a graded state.

Centrifugal methods, in which control of the centrifugal speed, centrifugal time, and viscosity produces a gradient, have been considered an effective way to produce FGMs[9, 10].The density difference between the matrix and the grading agent is considered to be the main factor in forming the gradient by this method. In general, the greater the density difference between the matrix and the grading agent, the easier the centrifugation process is; in the VGCF/polymer case, compared with the metal or the ceramics, the lower specific gravity of both the matrix and the VGCF is the main problem. Epoxy resins, which are one of the lightest thermosetting polymer matrixes used in industry, have excellent mechanical properties and electrical insulation, and are considered to be appropriate candidate polymer matrixes for creating VGCF/polymer FGMs.

In this work, we aimed to advance research in this field by fabricating VGCF-incorporated FGMs, and then studying the tribological, electrical and microwave absorbing behaviors of the FGMs; the optimum processing parameters were determined.

2.2 Experimental

2.2.1 Materials and Preparation

An epoxy resin (bisphenolA, JER 827, Japan Epoxy Resins Co., Ltd.),an anhydrous saturated aliphatic cyclic acid (HN5500, Hitachi Chemical Co., Ltd), and imidazole as a curing accelerant (EK BMI-12, Japan Epoxy Resin Co., Ltd.),in ratios of 100:85:1 were used. The density was 1.185 g/cm^3, the viscosity under room

temperature is about 1088mpa·s, and the glass-transition temperature (Tg) was about 164 °C.VGCFs (density: 2.0 g/cm^3, diameter: 150 nm, length: 10–20 μm; Showa Denko K.K.) were used as the grading agent. First, to solve the aggregation problem, the VGCFs were pre-dispersed in a hardener by sonication for 30 min at 55°C.They were then mixed with the epoxy resin, followed by mechanical stirring at an ultrahigh rotation speed of 18000 rpm[11] for 10 min and de-aeration for 15 min. A material containing 0.75 vol% VGCF was thus obtained. The experiments were conducted at room temperature and the centrifugation speed was varied from 1000 rpm to 3000 rpm with a constant centrifugation time. In order to study the effect of centrifugation time on the VGCF distribution in the matrix, for each centrifugation speed, centrifugation times of 30 min and 60 min were used. The samples were then cured and cut. The sample slices were obtained by cutting perpendicular to the direction of the centrifugal force, and were used for investigation of the FGM properties. The process is shown in Fig. 2-1.

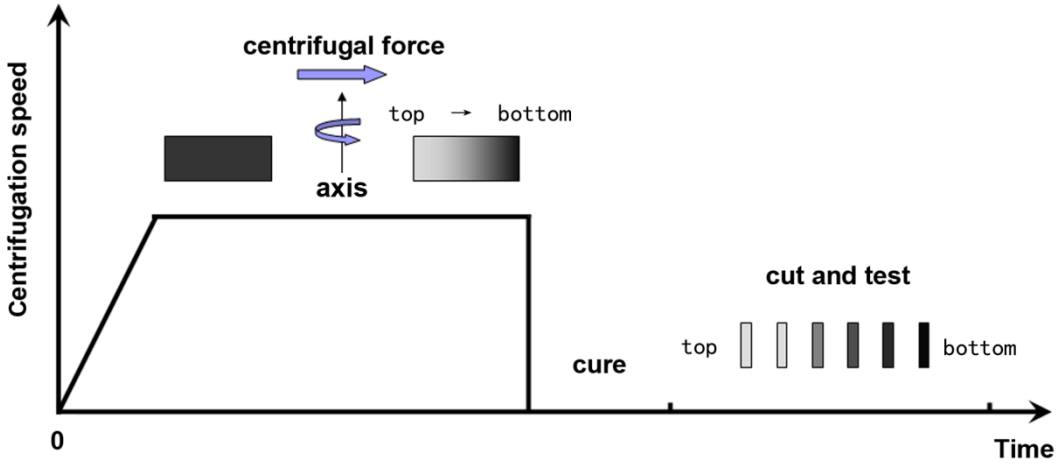

Fig. 2-1. Schematic diagram of preparation of FGM samples.

2.2.2 Characterization

The densities of the slices were determined (SMK-301, Shimadzu, AW/AX/AY series) to calculate the volume fractions. The arrangements of the VGCFs in the surfaces of the FGM slices were examined using a Hitachi S-5000 field-emission scanning electron microscope (FE-SEM) at an accelerating voltage of 20kV. The samples were fractured under the room temperature, then observed after sputter coating with Pt–Pd. The sliding friction properties were measured using a ball-on-plate-type surface measurement machine (TRIBO station, Type 32, Shinto Scientific, Japan), in which the FGM specimen was fixed on a plate that moved left and right along a horizontal linear path. A steel ball (SUS 304, diameter 10 mm) was used as the counterpart and held in a clamp at the end of a movable cantilever beam. The reciprocating friction stroke was 10 mm, and the tests were conducted under a normal load of 2 N. The average sliding speed was 10mm/s (2 s per cycle) and the number of cycles was 500.All measurements were carried out under ambient conditions without lubricants. The tangential drag force on the steel ball was recorded during the sliding friction test. The peak values in two directions were divided by the normal load to obtain the friction coefficient. Dynamic mechanical analysis was performed at a frequency of 10 Hz frequency in tensile mode at a 0.5% constant strain using a DVA-225 instrument (ITK, Japan). The temperature range was 75–210 °C, with a heating rate of 2 °C/min. The sample dimensions were20×4×1 mm^3 (length×width×thickness). A digital microscope (VHX1000, KEYENCE) was used to obtain two- and three-dimensional images of the worn FGM surfaces. The mean value was used as the volume resistance (Hiresta UP Model MCP-HT450, Mitsubishi Chemical Analytech Co., Ltd.).The samples used for measurement of microwave absorption properties is made

into a toroidal shape with an outer diameter of 7 mm, inner diameter of 3.0 mm and a thickness of 2 mm. The complex permittivity and permeability of the compound samples were measured using a vector network analyzer (37247D Anritsu Co., Ltd.) over a range of 0.5–10 GHz, and the reflection loss was calculated from the measured complex permittivity and permeability.

2.3 Results and Discussion

2.3.1 VGCF Distribution

Fig. 2-2 presents the volume fractions of VGCFs in the FGM slices. An average density value of five measurements is reported for a particular sample. The volume percentage of fibers was determined using the following formula [12]:

$$V_{VGCF}\% = \left[1 - \left\{\left(\rho_{VGCF} - \rho_c\right)/\left(\rho_{VGCF} - \rho_{EP}\right)\right\}\right] \times 100 \quad (1)$$

where $V_{VGCF}\%$ is the volume percentage of VGCFs in the FGM, ρ_{VGCF} is the VGCF density, ρ_c is the density of the FGM slice, and ρ_{EP} is the epoxy resin density.

The results show that the volume content of VGCFs in the epoxy substrate increased as a function of the normalized thickness along the centrifugal force direction, which confirmed a gradient. With increasing centrifugation speed, the maximum volume content of VGCFs in the FGM reached 1.9 vol% and 2.4 vol% for centrifugation times of 30 min and 60 min. The results also showed the structural details of the composite produced. Centrifugation of the FGM for 30 min at a centrifugation speed of 1000 rpm did not produce a large gradient in the fiber distribution. However, on increasing the speed from 1000 rpm to 3000rpm, a linear increase in the VGCF content along the centrifugal force direction was detected.

When the centrifugation time was increased to 60 min, a much larger gradient was produced; however, in the case of centrifugation at 3000 rpm, the centrifugal force was so strong that most of the VGCFs were deposited at the bottom of the sample, and closely packed, whereas the top of the sample was virtually free of VGCFs. The middle layer almost vanished under these preparation conditions. In particular, for a centrifugation speed of 1000rpm, the volume fraction at the normalized thickness of 0.2 was relatively high; this was considered to be an error and did not confirm the grading tendency. Based on the filler distribution in the FGMs, the sample produced at 2000 rpm for 60 min was the most uniformly graded. This sample was investigated using FE-SEM. The friction coefficients and the electrical properties of the FGMs were studied, dynamic mechanical analysis was performed, and the gradients of the mechanical and electrical properties were confirmed. In the FE-SEM image,(Fig. 2-3), the white line is the VGCFs dispersed in the epoxy resin. The VGCF content gradually increased from the top to the bottom of the image, which also indicates that a gradient was formed. The image confirms that the VGCF was well dispersed in the epoxy resin.

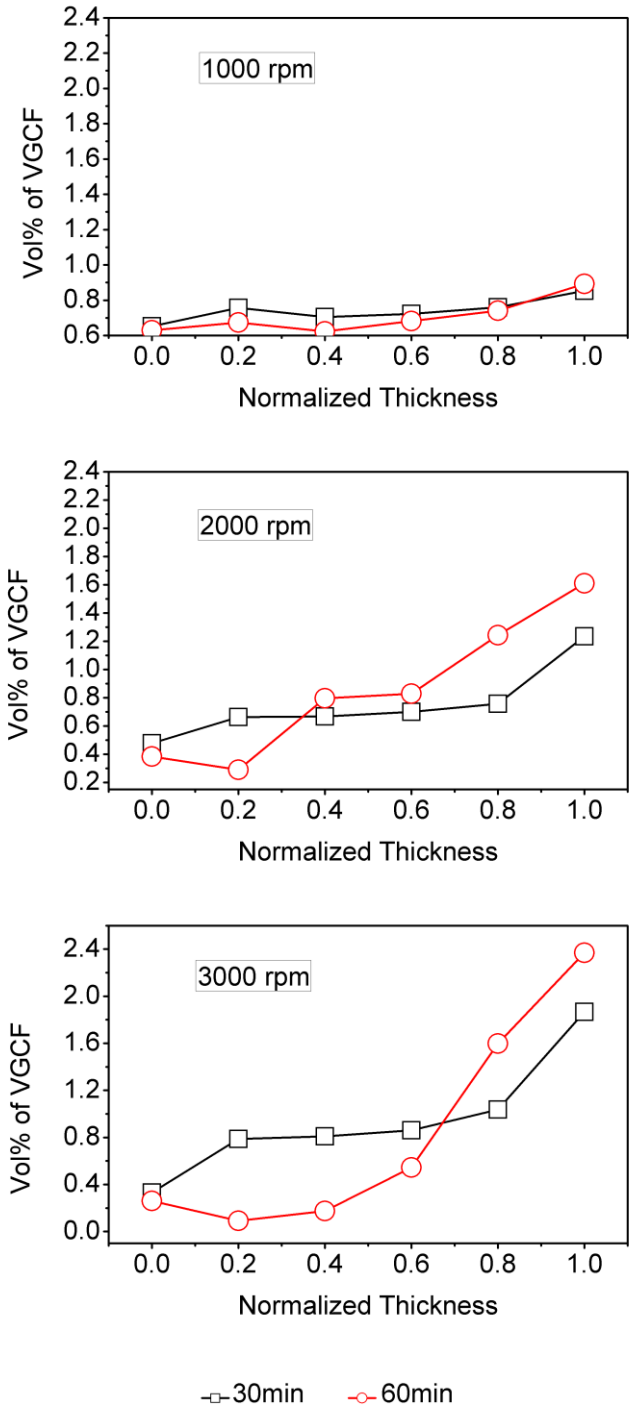

Fig. 2-2. Volume content distribution of VGCF with composite thickness.

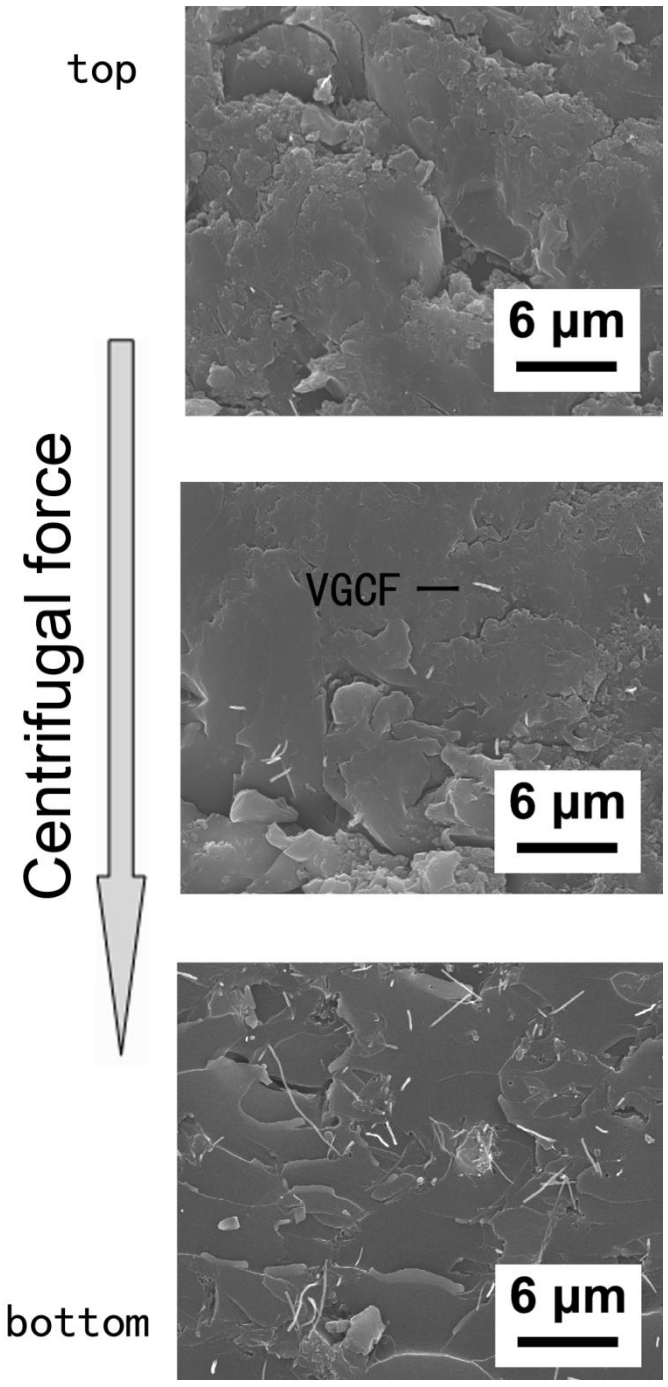

Fig. 2-3. FE-SEM image of fracture surface of selected sample.

2.3.2 Tribological Behavior

There are some technical applications, such as in gears, in which it is useful to have different properties at different locations in the cross-section of the component. This could be a higher hardness and sliding resistance on the outside, and higher toughness and damage tolerance at the inside. Also, sudden property jumps, for example, in hard coatings, are undesirable, since these can cause stress singularities at interfaces, associated with local coating failure as a result of spalling-off effects. For these purposes, the creation of a filler distribution gradient is an effective way of preparing wear resistant materials [13–17].

Fig. 2-4shows that with increasing VGCF content in the FGM, the friction coefficient of the FGM effectively decreased. Two friction coefficient directions in the FGMs were used for the sliding tests. The running stage was considered to be up to 200 cycles. As the stick–slip motion was repeated during sliding friction, stable abrasion patterns, i.e., a series of parallel ridges perpendicular to the sliding direction (Fig. 2-4), were formed, resulting in a stable value of the friction coefficient. In this work, we took a normalized thickness of 0.0 as the top position of the FGM, 0.4 as the middle position, and 1.0 as the bottom position. The pure epoxy resin had a friction coefficient less than 0.2, which is similar to that of the top slice of the FGMs. Along the centrifugal force, the friction coefficient of the middle part decreased to about 0.1, and the friction coefficient of the bottom slice decreased to 0.05, i.e., as the VGCF concentration increased to 1.6 vol%, the friction coefficient of the FGM decreased to 25% that of the original value. These results indicate that self-lubrication of the VGCF/epoxy FGMs contributed to the reduction in the friction coefficient. Also, a gradient in the sliding properties of the FGMs was confirmed. The worn

surface was then investigated using a digital microscope (Fig. 2-5). In the Fig. 2-5, the white part represents the damaged surface, we can see that the worn surface of the pure epoxy resin (left) is much rougher than that of the bottom of the FGM incorporating a large amount of VGCFs (right). From top side to bottom side of the FGMs, the surface become less damaged, and for the bottom side of the FGMs, the results show no severe damage to the surface.

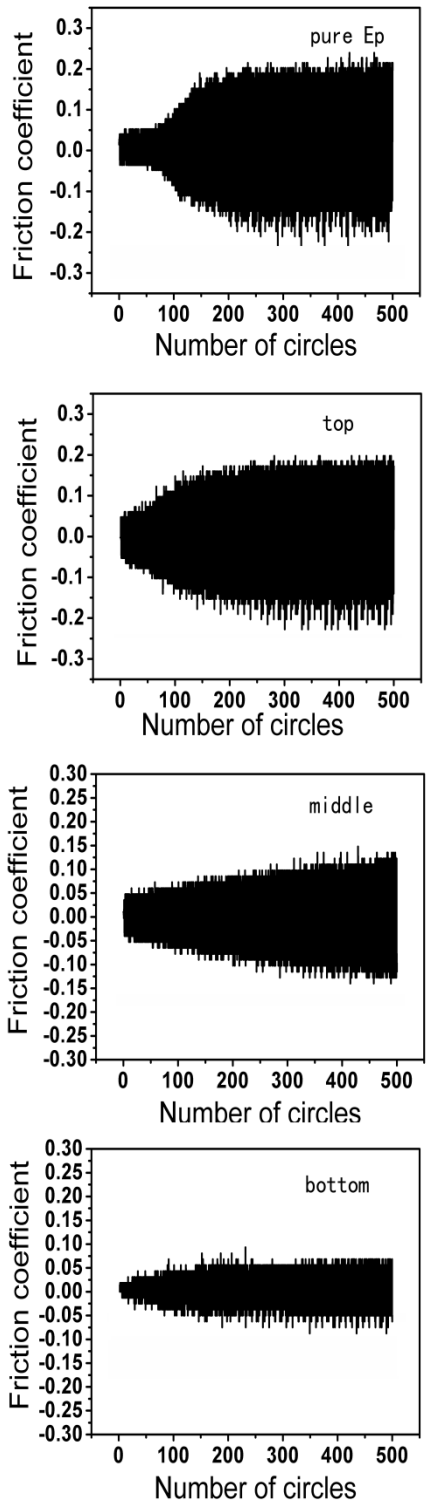

Fig. 2-4.Friction coefficient of VGCF/epoxy FGM as a function of number of cycles along the centrifugal force direction (from top to bottom).

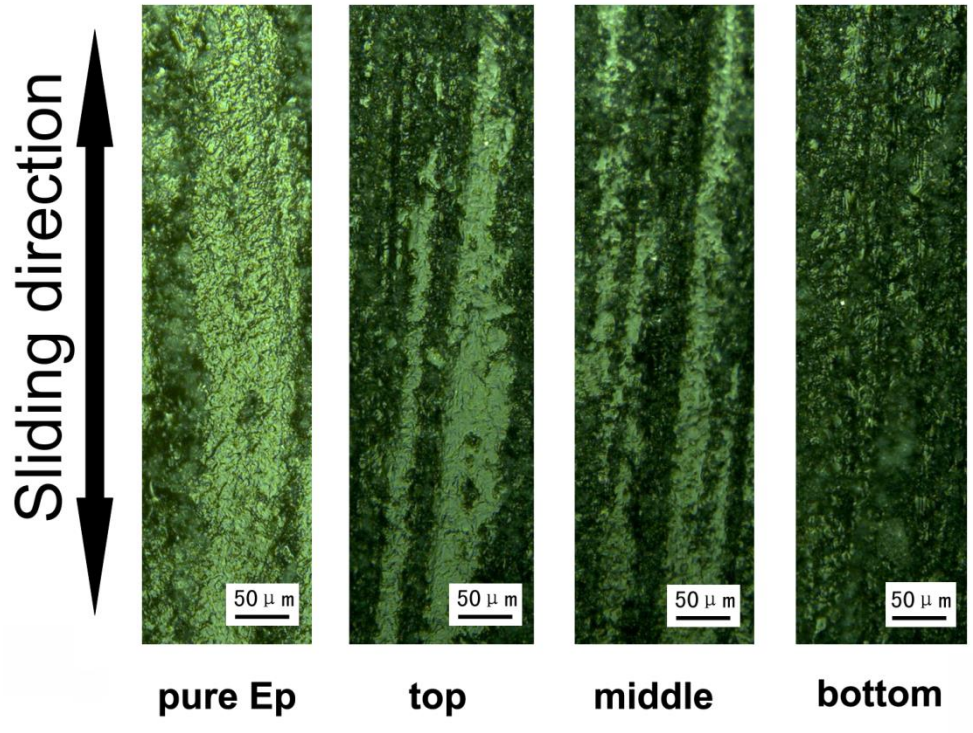

Fig. 2-5. Two-dimensional microscope image of worn surface.

2.3.3 Viscoelastic Properties

Because sliding friction is closely related to the viscoelastic properties of polymers, it is important to investigate the dynamic mechanical properties to study the low friction coefficients of the FGMs [18–20]. Fig.2-6shows the storage modulus and viscous dissipation as a function of temperature from 75 to 210 °C. At around the *T*g which is about 164 °C, the storage modulus decreased suddenly because the FGMs have been transformed to a soft state. Also, a graded modulus is obviously seen from the top to the bottom of the FGM slice. With increasing VGCF content, the viscous dissipation decreased at the *T*g, and as the VGCF concentration in the slice increased, the *T*g increased gradually (shown in the inset). These results suggest that the gradient of the *T*g and the loss factor contribute to formation of a gradient in the friction coefficient.

2.3.4 Electrical Properties

Electrical property is a very important factor to the microwave absorbing behavior, the in-situ-measured volume resistance (Fig. 2-7) exhibited a depth-graded distribution in the matrix because the electrical conductivity of the FGM nicely followed the grading direction; In the Fig. 2-7a, the top side of FGMs shows the volume resistance value near $10^{14}\Omega\cdot$cm, along the normalized thickness, the value gradually down to $10^{7}\Omega\cdot$cm at the middle position of 0.4, then suddenly became $10^{3}\Omega\cdot$cm at position of 0.6, which turned to the conductive state. In the Fig. 2-7b, we change the horizontal axis from normalized thickness to concentration of VGCF, it was found that when the VGCF content reached 0.8 vol% in the composites, a significant decrease in the volume resistivity appeared as a result of the formation of

conductive pathways in the nanocomposites at the percolation threshold.

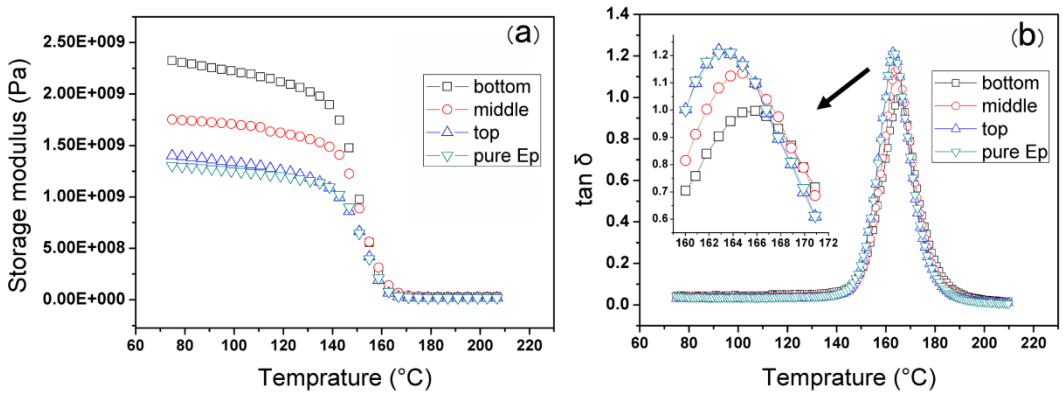

Fig. 2-6. Dynamic mechanical properties of VGCF/epoxy FGM as a function of temperature: (a) storage modulus and (b) loss factor.

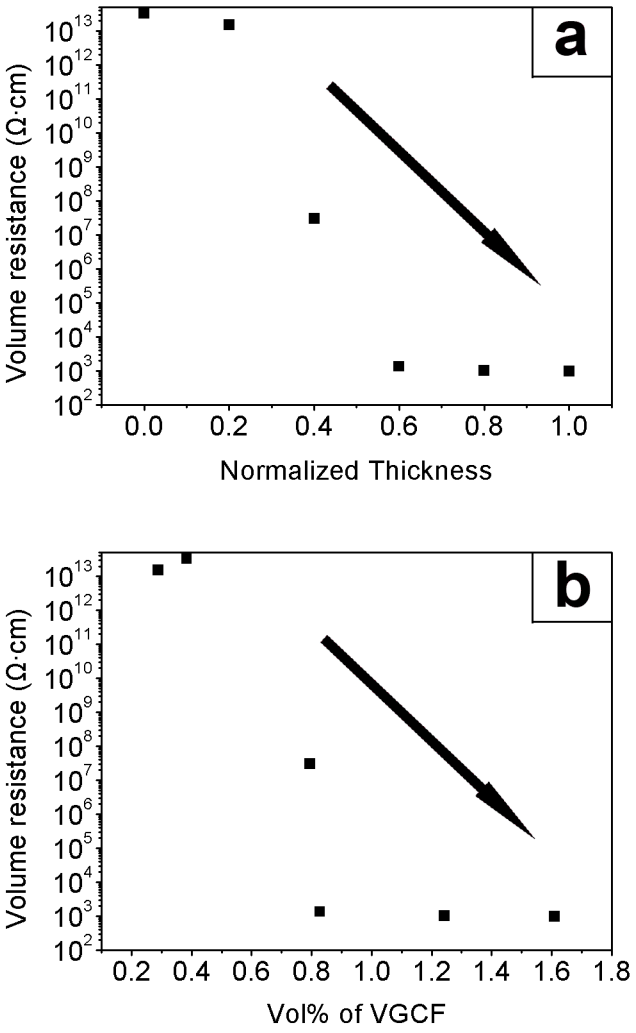

Fig. 2-7. Volume resistance distribution of VGCF with: (a) composite thickness and (b) volume fraction of VGCF.

2.3.5 Microwave absorption properties

For a good absorbing material, there are two requirements: first, the intrinsic impedance of material is made equal to the impedance of free space. Second, the incident electromagnetic wave must enter and be attenuated rapidly through the material layer. Therefore, the uniform structure material can be improved by designing the gradient structure to fulfill the conditions [21], and thus we investigated the absorption properties.

Fig. 2-8 shows the real and imaginary parts of the complex permittivity of the FGMs and the pure epoxy. The real part of the complex permittivity is related to the stored energy within the medium while the imaginary part is related to the dissipation (or loss) of energy within the medium. As shown in Fig. 2-8, compared to pure epoxy, both the real part and imaginary part of the permittivity of the FGM samples increases with the VGCF content from top to bottom, especially in the range of 0.5-7 GHz. Between 7 and 10 GHz, the permittivity is less sensitive to the VGCF content. It is also found that the permittivity is critically dependent on the frequency and decreases in inverse proportion to the frequency.

To investigate the intrinsic reasons for microwave absorption of FGMs, the dielectric loss factor and the magnetic loss factor of bottom sample were calculated. The results in Fig. 2-9 shows frequency dependence of the loss tangent of dielectric/magnetic of FGMs. It is observed that the value of dielectric loss is much higher than that of magnetic loss especially in the range of 0.5-8 GHz. It suggests that microwave absorption enhancement of the FGMs results mainly from dielectric loss rather than magnetic loss.

The reflection loss (R.L.) of the FGMs sample with thickness of 2mm in 0.5-10 GHz

was calculated, as shown in Fig. 2-10, according to transmission line theory[22], as:

$$R.L. = 20 \log \left| \frac{Z_{in}-1}{Z_{in}+1} \right| \quad (2)$$

$Z_{in}$is the normalized input impedance of a metal-backed microwave absorbing layer.

$$Z_{in} = \sqrt{\frac{\mu_r}{\varepsilon_r}} \tanh \left[j \left(\frac{2\pi fd}{c} \right) \sqrt{\mu_r \varepsilon_r} \right] \quad (3)$$

where f is the microwave frequency in Hz, d is the thickness of the absorber in m, and c is the velocity of light in free space in m/s.

It is obvious that microwave absorption varies from the different contents of VGCFs. The bottom of the FGMs exhibits the best microwave absorbing property. The minimum reflection loss of bottom sample is about -4dB at 10 GHz when d= 2 mm represents the best absorbing property. The results indicate that the grading process lead to a VGCF content change in dielectric, significantly affecting the microwave absorption behavior.

The relationship between reflection loss and reflectance (R) can be illustrated as Eq. (4) [21], and the value of reflection is minus. In this work, from top to bottom of the FGMs, the value of reflection loss of the materials goes smaller, according to the Eq. (4), the reflectance become larger, so the value of topside's reflectance is the smallest, thus the microwave can go deeper into the FGMs, and can be absorbed by the VGCF more than the uniform structure materials.

$$R.L. = 10\log(1-R) \quad (4)$$

For this reason, the gradient structure is suggested to be a better design for microwave absorbing material.

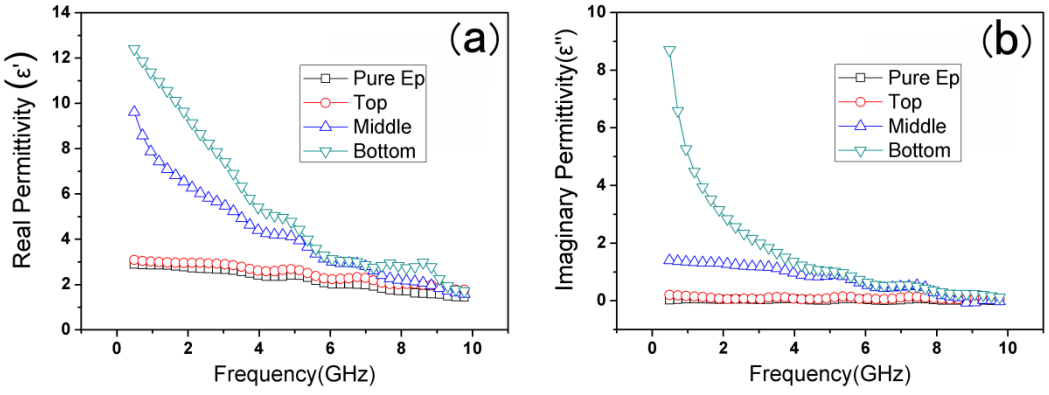

Fig. 2-8. Real part (a) and imaginary part (b) of permittivity of FGMs and pure epoxy.

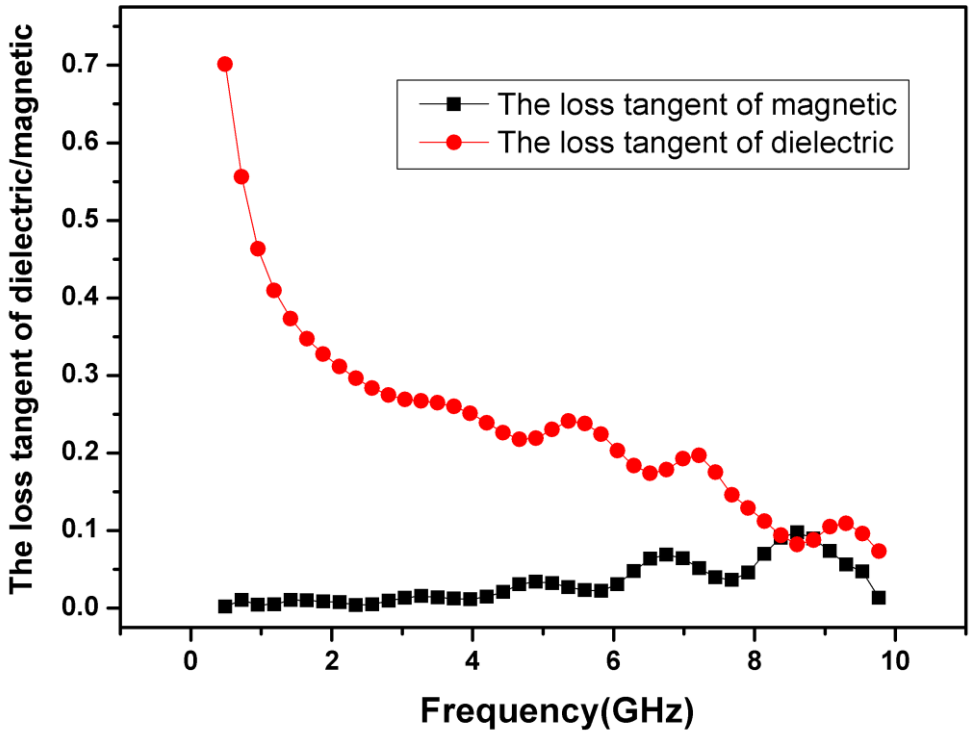

Fig. 2-9. Frequency dependency of loss tangent of dielectric/magenetic of bottom side of FGMs.

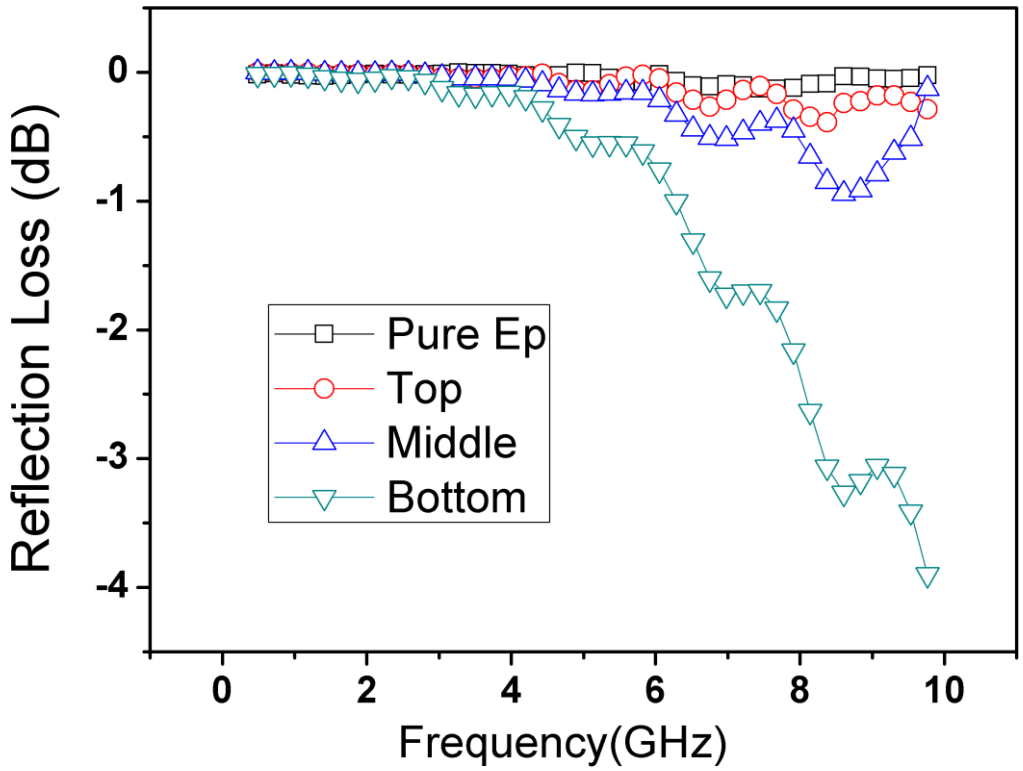

Fig. 2-10. Reflection loss curves for FGMs and pure epoxy with 2 mm thickness in the frequency range of 0.5-10 GHz.

2.4 Summary

In summary, we successfully produced VGCF-incorporated polymer-based FGMs using the centrifugal method. The gradual VGCF incorporation within an epoxy resin effectively caused depth gradients in the tribological behavior, electrical conductivity and microwave absorption properties of the FGMs. The VGCF grading capability indicated that it is possible to tailor desired gradient filler content distributions by careful selection of the processing parameters, thus precisely controlling variations in the properties and microstructure. The FGMs fabricated in this work may applied to some special area. For instance, the friction coefficient gradients of the FGMs would enable the development of some technical applications, e.g., gears or rollers, in which a high sliding resistance on the outside is needed. The gradients in electrical conductivity can be considered to be ideal for applications demanding an electrically conductive surface and an insulating core for FGMs. As for the microwave absorbing material, the graded structure may be a better design.

These achievements strongly suggest that nanosized carbon materials could be employed as novel multifunctional materials for manipulating and designing multi-FGMs within conventional polymer materials. And it is promising for use in a variety of new and challenging structural, electronic, and military applications, and may open up further areas for intensive exploration and research.

Reference

1. M.Koizumi and M.Niino, MRS. Bull., 20 (1995) 19.

2.C.Klingshirn and M.Koizumi,J. Mater. Sci. Lett., 19(2000) 263.

3.S.A.R.Hashmi and U.K.Dwivedi, Polym.Eng. Sci., 46(2006) 1660.

4. N. Chand and A.M. Naik, Polym. Compos.,29(7) (2008) 736.

5.C.R,Choe and C.Klingshirn, Macromol.Res., 10(2002) 236.

6.M.KrumovaandC.Klingshirn, Compos.Sci. Technol., 61(2001) 557.

7.Y.K.Choi, K.Sugimoto and S.M.Song, Carbon, 43(2005) 2199.

8. J.M.Ting,J. Mater.Sci., 34(1999) 229.

9.Y.Watanabe, N.Yamanaka and N.Fukui, Compos. PartA,29A(1998) 595.

10.R.Rodiguez-Castro and M.H.Kelestemur, J. Mater. Sci., 37(2002) 1813.

11. X.Z. Xu, A.J. Uddin, K. Aoki, Y. Gotoh, T. Saito, M. Yumura, Carbon, 48(2010) 1977.

12. M. Krumora, C. Klingshirn, F. Haupert, and K. Friedrich, Compos. Sci. Technol., 61(2001) 557.

13. M. Funabashi, Composites Part A, 28A (1997) 731.

14.E.J. Vinarcik, SAMPE. J.,34 (1998) 40.

15.N.J. Lee, J. Jang, M. Park, and C.R. Choe, J. Mater. Sci.,32(1997) 2013.

16.C. Klingshirn, M. Koizumi, F. Haupert, H. Giertzsch, and K. Friedrich, J. Mater. Sci. Lett.,19 (2000) 263.

17. C. Choe, C. Klingshirn, and K. Friedrich, Macromol Res., 10(4) (2002) 236.

18. W. Brostow, and H.E. HaggLobland, Polym. Eng. Sci., 48(2008) 1982.

19. H.X. Jiang, Q.Q. Ni, and T. Natsuki, Polym. Compos.,32(2011) 675.

20. W. Brostow, H.E. HaggLobland, and M. Narkis, J. Mater.Res.,21 (2006) 2422.

21. M.Chen, Y.Zhu, Y.Pan, H.Kou, H. Xu, and J.Guo, Mater. Design.,32 (2011) 3013.

22. S.S. Kim, S.B.Jo, K.I. Gueon, K.K. Choi, J.M. Kim, and K.S. Churn, IEEE Trans. Magn.,27(1991) 5462.

Chapter 3

Functionally Graded Epoxy Composites using Silane Coupling Agent Functionalized MWCNTs under Relative Low Viscosity Environment

Functionally Graded Epoxy Composites using Silane Coupling Agent Functionalized MWCNTs under Relative Low Viscosity Environment

3.1 Introduction

The concept of functionally graded materials (FGMs), proposed in Japan in 1984, was first applied to the design of super heat-resistant materials for spacecraft, and was then developed rapidly in many other challenging areas. By grading the components in a matrix material to combine entirely different materials, their unique structures can be combined in such a way that the breakages that typically occur at their interface can be avoided or alleviated [1–4]. Not only metals and ceramics but also polymers have been used as matrices to prepare different types of FGMs. Polymer matrices have advantages in their low cost, erosion resistance, and lightness compared with metals and ceramics. With the development of processing technologies, polymer FGMs have been prepared for different purposes using a number of methods [5–9]. For example, in a priority program project, Klingshirn et al. [10] used two resins as matrix materials, and SiC particles, aramid particles, glass fibers, and carbon fibers as filler materials. Rings and tubes with a gradient in their filler contents were produced by centrifuging a dispersion of particles in the resin prior to hardening. A polymer with a discrete variation in plasticizer content was cast by Parameswaran et al. to study crack propagation [11]. However, to develop advanced FGMs with excellent properties and multiple functions, nanofillers were introduced as the grading agent because of their remarkable properties and multiple applications. An example of such a material is carbon nanotubes (CNTs) [12-13].

CNTs have been employed as extremely strong nano reinforcements to produce composites showing extraordinarily high strength, even at low CNT contents. However, there have been very few studies investigating the fabrication of CNT-reinforced FGMs to date. Hansang Kwon et al. designed gradient layers to fabricate CNT-reinforced aluminum-matrix FGMs using a powder metallurgy route. Estili et al. reported a CNT gradient layer in ceramic matrix composite materials fabricated using a spark plasma sintering process [12-13]. Even so, most other studies that have investigated CNT-reinforced FGMs were based on numerical calculations or modeling. This is mainly because of a lack of appropriate processing technologies to synthesize the composites from the homogenous to graded states using nano-agents. Furthermore, nanofillers can be difficult to disperse in polymer resin due to the relatively small difference between their weight densities, and often show weak interfacial bonding with the polymer matrix [14].

In this study, MWCNTs were used as a reinforcing agent to prepare polymer matrix FGMs using a centrifugation method by controlling the centrifugal speed, centrifugal time, and viscosity [15-16]. Epoxy was selected as the matrix because of its excellent mechanical and electrical insulation properties, lightness, and low cost [17]. The introduction of silane coupling agents to modify the MWCNTs is considered to be an effective way to improve the dispersion of MWCNTs in a polymer during this process [18-19, 38-40]. Before the preparation of the polymer matrix FGMs, the MWCNTs were first oxidized in concentrated nitric acid to produce surface hydroxyl groups. The silane agent was then grafted on the surface of the MWCNTs in a dehydration condensation reaction.

We hope to use these MWCNT-epoxy FGMs in novel applications. For example, it

could be applied as a wear-resistant material possessing a high wear resistance at its surface without the interfacial problems associated with coated materials. Materials with a gradient in conductivity would be ideal for applications demanding an electrically conductive surface and an insulating core. The investigation of the microwave absorption behavior of the FGMs in this work indicates that structural grading can lead to a graded absorption ability, which may make it possible to design better microwave absorption materials.

In this work, we focused on solving the MWCNT aggregation problem to produce higher quality FGMs, and aimed to improve the fabrication process for MWCNT-reinforced FGMs.

3.2. Experimental

3.2.1. Materials and Preparation

Modification of MWCNTs. The modification of the MWCNTs (40–70 nm, Wako Pure Chemical Industries, Japan) was accomplished in two steps (shown in Fig. 3-1); hydroxyl groups were grafted on the surface of the MWCNTs using concentrated nitric acid (69wt%, Wako Pure Chemical Industries, Japan), and were then modified using a silane coupling agent(Z6020, Dow Corning Toray Co., Ltd.). The chemical name of silane is N-(β-aminoethyl)-γ-aminopropyltrimethoxysilane. In the first step, the surface of the MWCNTs was oxidized using nitric acid. The details of procedure were as follows. First, 0.5 g of MWCNTs was dispersed in 70 mL nitric acid in a three neck flask followed by magnetic stirring at 120°C in an oil bath for approximately 12 h. Repeated washing with water and ethanol was then performed, followed by vacuum drying, to obtain the oxidized MWCNTs. In the second step, the

silane coupling agent diluted in 5vol% pure water in ethanol to make a 1wt% solution. The amounts of coupling agent (%) added were based on the weight percent of filler used. The ethanol solution was magnetically stirred in a beaker, and the silane was added slowly to ensure uniform mixing. The MWCNTs were then added slowly and stirred continuously for 10 min, after which the reaction proceeded for 2 h under sonication. The modified MWCNTs were then dried at 100°C for 5 h to allow the complete evaporation of ethanol.

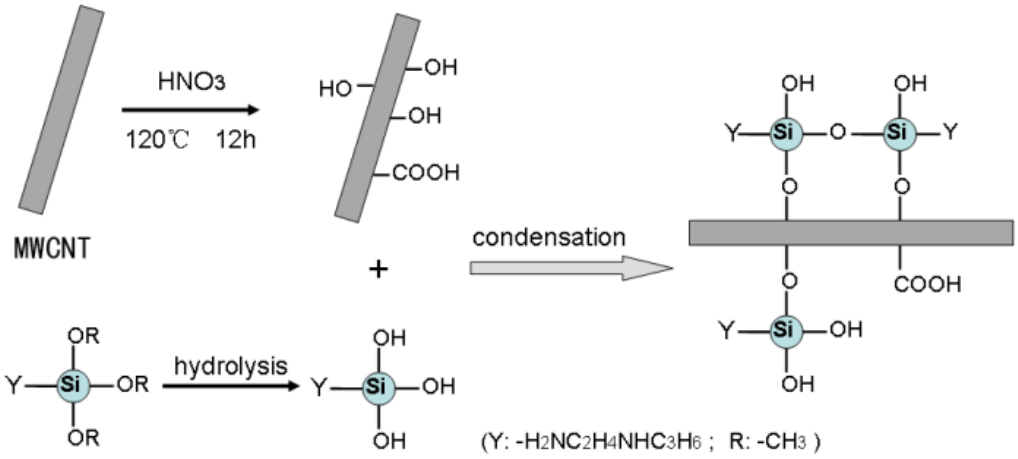

Fig. 3-1. Mechanism of silanization for the nano-MWCNTs.

After the silanization of the MWCNTs, it is used to prepare the FGMs by the centrifugal method. the modified MWCNTs (s-MWCNTs) were better dispersed in the epoxy due to the reaction of anchoring of the silane units from the silicon atoms side as well as from the organic moieties which happened directly during the curing stage.

Preparation of MWCNT/Epoxy FGMs. An epoxy resin (Denatite XNR 6815, JER 827, Nagase Chemtex Co., Ltd.) mixed with a curing agent (Denatite XNH 6815, Nagase Chemtex Co., Ltd.) at a weight ratio of 100 to 27. The epoxy resin is bisphenolA type, the hardener is modified cycloaliphatic polyamine Isophoronediamine. The density was approximately 1.14 g/cm3.The viscosity is about 260mpa·s. s-MWCNTs were used as the grading agent. To ensure the uniform dispersion of the filler, the MWCNTs were first pre-dispersed in the epoxy resin using sonication for 30 min at 55°C followed by mechanical stirring at an ultrahigh rotation speed of 18,000 rpm for 10 min; this was followed by15 minutes of deaeration[20].A 1wt% MWCNT material was produced using the centrifugal method. We used the viscosity as the constant parameter for the experiment, which was conducted at room temperature. For the centrifugation parameter, the optimum condition is under about 2000 rpm and 60 minutes. The samples were then cured and cut perpendicular to the direction of the centrifugal force to obtain sample slices; these samples were used to investigate the properties of the FGMs. The whole process is illustrated in Fig. 3-2.

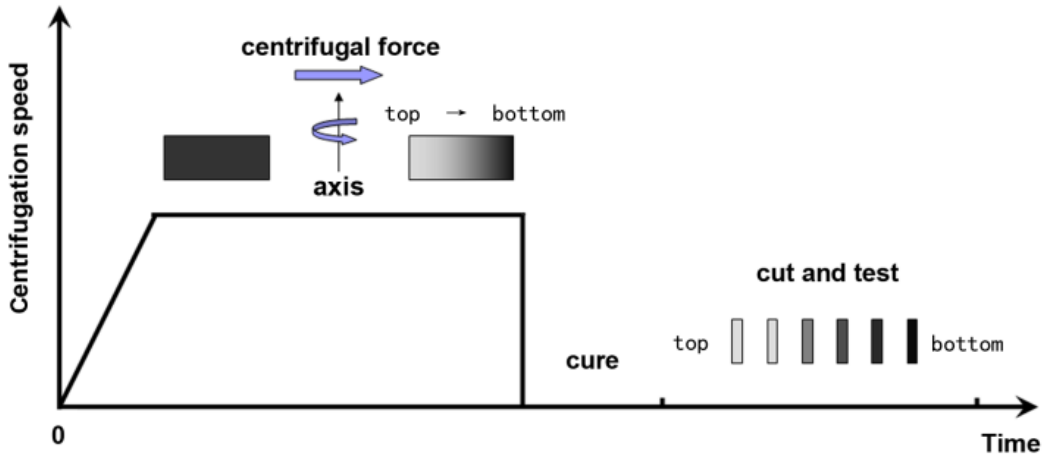

Fig. 3-2.Schematic diagram of the FGM sample preparation procedure.

3.2.2 Characterization

Pristine MWCNTs, oxidized MWCNTs, and s-MWCNTs were visualized using a Hitachi S-5000 field emission scanning electron microscope (FE-SEM). X-ray photoelectron spectroscopy (XPS) analyses were performed on a Kratos Axis Ultra DLD X-ray photoelectron spectrometer with a standard Mg Ka (1256.6 eV) X-ray source operated at 10 mA and 15 kV. All binding energies were referenced to Au (4f7/2) at 84 eV. Raman spectroscopy was carried out using a Kaiser Holo-Lab 5000 series spectrometer furnished with a 514nm-excitation laser. Fourier transform infrared spectra (FT-IR) were recorded on a Shimadzu Irprestige-21 spectrometer in the range 400–4000 cm–1, using the KBr method. The density (SMK-301, Shimadzu, AW/AX/AY series) of the slices was investigated. Dynamic mechanical analysis was performed at a frequency of 10 Hz, in tensile mode at a 0.5% constant strain, using a DVA-225 instrument (ITK, Japan). The temperature range was 0–120°C, with a heating rate of 2°C/min. The sample dimensions were 20×4×1 mm3 (length×width×thickness). The volume resistance of the FGMs slides was measured at 10 different locations on each sample using a resistivity meter (Hiresta UP Model MCP-HT450, Mitsubishi Chemical Analytech Co., Ltd). The mean value was used to represent the volume resistance. The samples used for measurement of microwave absorption properties were formed into a toroidal shape with an outer diameter of 7 mm, inner diameter of 3.0 mm and a thickness of 2 mm. The shielding effectiveness and the complex permittivity and permeability of the compound samples were measured using a vector network analyzer (37247D Anritsu Co., Ltd.) over a range of 0.5–10 GHz, and the reflection loss was calculated from the measured complex permittivity and permeability.

3.3. Results and Discussion

3.3.1. Analysis of s-MWCNTs

FE-SEM analysis.

Fig. 3-3 shows typical FE-SEM images of MWCNTs before and after the acid and silane treatment. The pristine MWCNTs exhibit apartially bundled morphology and amorphous impurities. The acid-treated a-MWCNTs show an obvious reduction in amorphous nanoparticles and bundled MWCNTs in comparison to the pristine MWCNTs. The a-MWCNTs showed no obvious shortening or damage, and the s-MWCNTs showed no obvious entanglement. The s-MWCNTs were more easily dispersed than the a-MWCNTs, because the electron interactions and surface energy of the s-MWCNTs were reduced by the breaking of the π bonds on the MWCNT surface, which was grafted with long macromolecular chains.

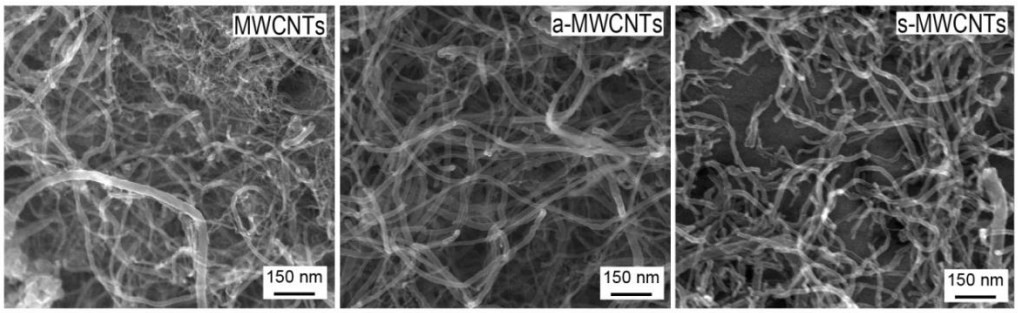

Fig. 3-3.FE-SEM images of pristine MWCNTs, a-MWCNTs, and s-MWCNTs.

XPS analysis.

XPS measurements were carried out to determine the elemental composition of the s-MWCNTs. A typical XPS spectrum is presented in Fig. 3-4. Survey scans of the MWCNTs showed the presence of oxygen and carbon. In contrast to the pristine MWCNTs, the s-MWCNTs showed the existence of oxygen, carbon, nitrogen, and silicon, which indicated that the silanization of the surface of the MWCNTs was successful.

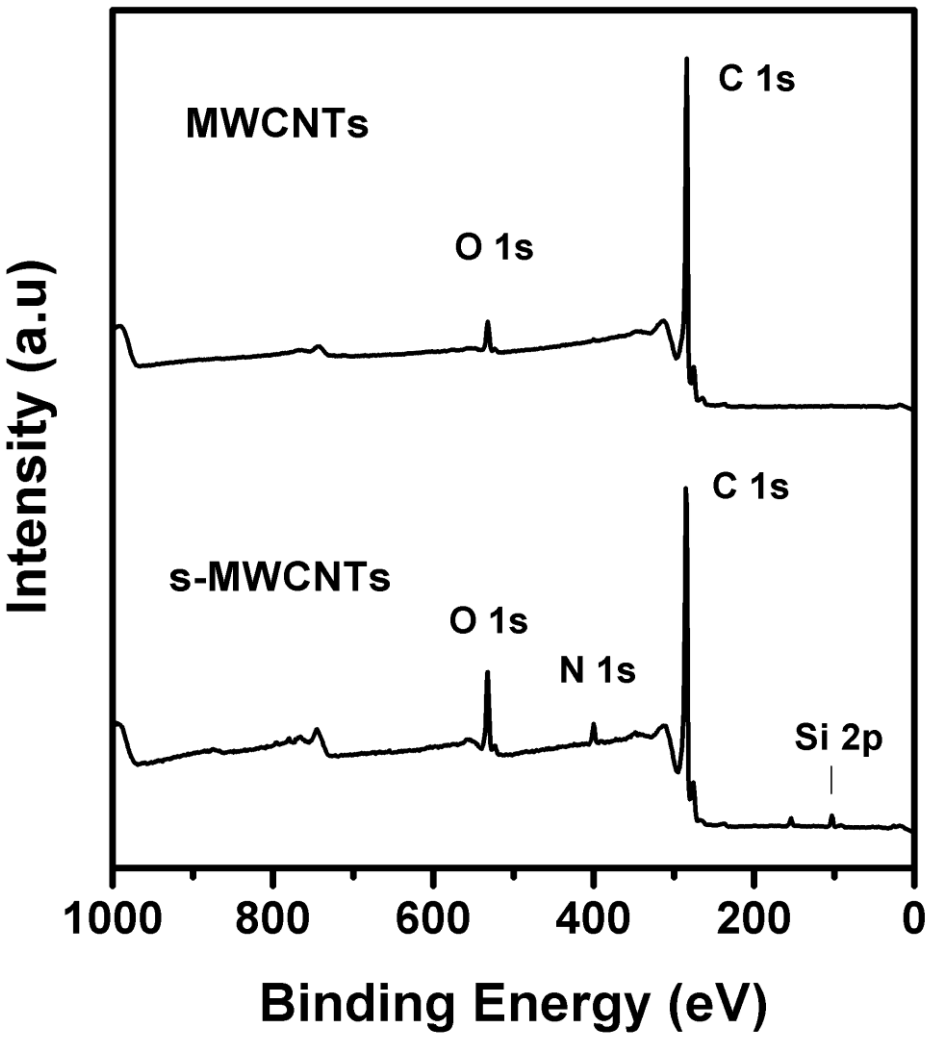

Fig. 3-4.XPS spectra of pristine MWCNTs and s-MWCNTs.

FT-IR analysis of the s-MWCNTs.

Fig. 3-5 shows FT-IR spectra for the pristine and silane-functionalized MWCNTs, measured in specific regions. The peak around 3380 cm–1 was assigned to the vibrational modes of the –OH groups, indicating the presence of functional groups on the s-MWCNTs.21 The silane treatment resulted in an increase in the peak intensity. The peak at 1370 cm–1 corresponded to C–H stretching vibrations.22 The peaks located at 2926, 2881, and 1409 cm–1 were attributed to the –CH vibration of the aminosilane attached to the MWCNT surface.23 The peaks at 1601 and 1499cm–1 were due to the deformation vibrations of NH2, and confirmed the presence of silane on the MWCNT surface.24 The appearance of new peaks at 1124 and 1024 cm–1was attributed to the presence of Si–O–Si stretching and Si–O–C stretching vibrations, respectively, further confirming that the dehydration polycondensation reaction had occurred between the silanes and the MWCNTs.19 The results described above indicated that the grafting of functional groups on the MWCNTs was realized using silanization, thus improving the dispersion of the MWCNTs in the epoxy resin.

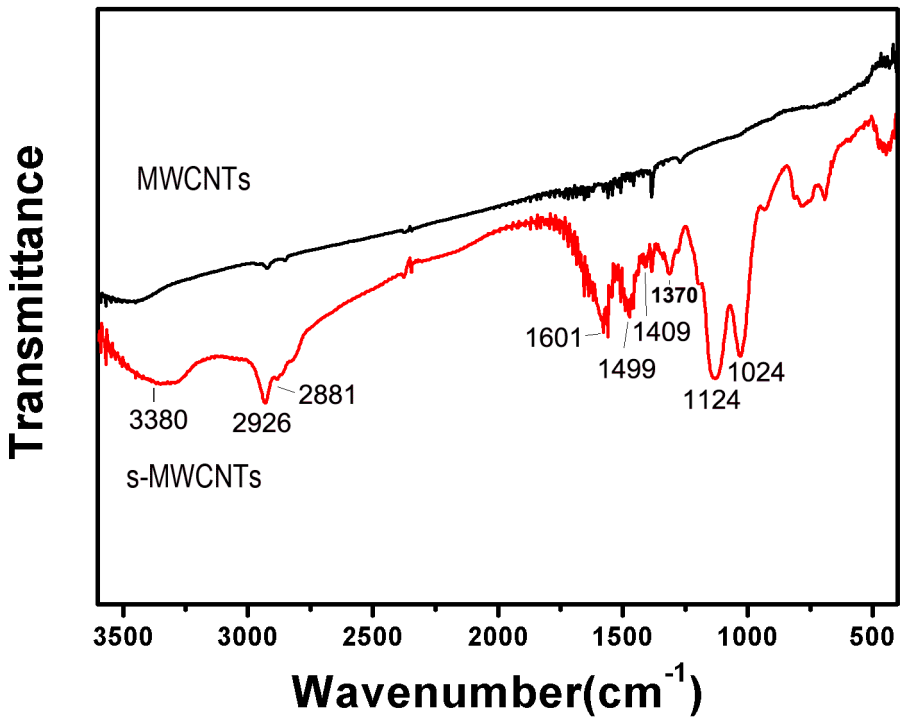

Fig. 3-5.FT-IR spectra of pristine MWCNTs and s-MWCNTs.

Raman analysis.

Raman spectroscopy, an important tool for the characterization of carbon materials,[25, 26] was applied to obtain structural information about the MWCNTs before and after the silane treatment. The two characteristic bands: the D-band (disorder band) at 1343cm–1, and the G-band (graphite band) at 1570cm–1 were observed in Fig. 6. The increase in the relative intensity of the D and G bands (ID/IG ratio) is often taken as confirmation of successful modification.[27, 28] The ID/IG intensity ratio increased from 0.69 (MWCNTs) to 0.95 (a-MWCNTs), implying the generation of surface defects due to the acid treatment. Similarly, the silane treatment (s-MWCNTs) further increased the (ID/IG) value to 1.02, indicating the presence of surface defects.

The increases in the ID/IG ratios for the s-MWCNTs confirmed the successful introduction of functional groups on the MWCNT surfaces. Besides the first-order D-band, the spectra of the samples also showed another first-order band at approximately 1604cm–1; this was assigned as a D'-band, a type of band that also indicates structural defects. The D'-band corresponded to a graphitic lattice mode with E2g symmetry.[27] As shown in Fig. 3-6, the intensity of the D'-band exhibited the same increasing tendency as the D-band, which was also attributed to the increase in the structural disorder after modification. Thus, the Raman analysis confirmed the successful introduction of functional groups onto the MWCNT surfaces, in good agreement with the XPS and FT-IR analyses.

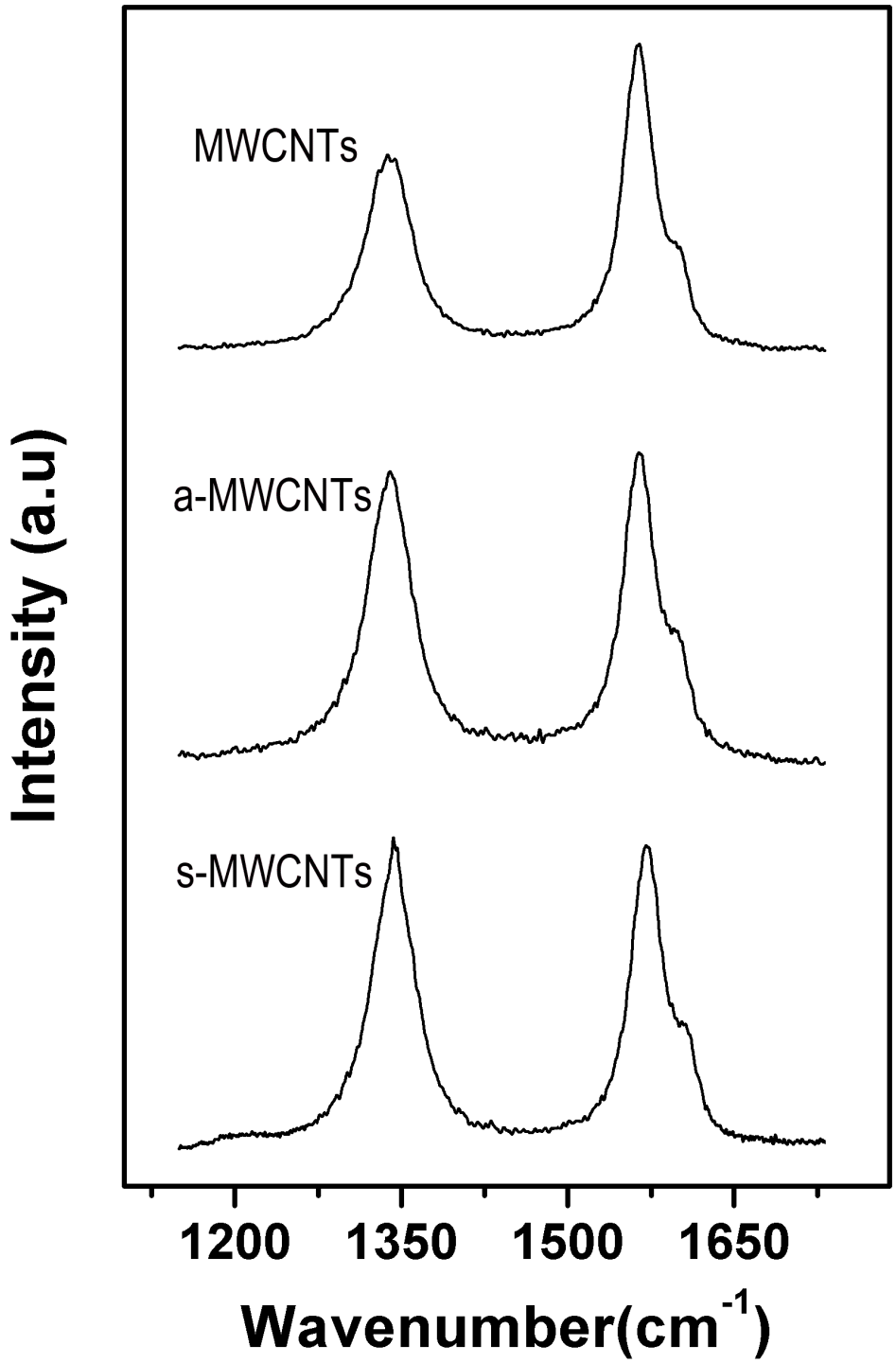

Fig. 3-6. Raman spectra of pristine MWCNTs, a-MWCNTs, and s-MWCNTs.

3.3.2. MWCNT Distribution

We believe that the aggregation of the pristine MWCNTs occurred in the epoxy curing stage because the viscosity became very low as the temperature increased. In this case, the nanoparticles would have aggregated more easily than they would under high viscosities. The density of each FGM slide was determined after the silanization of the MWCNTs. The results are shown in Fig. 3-7. Without silane treatment to the MWCNTs, the aggregation will lead to irregular properties of FGMs, on the contrary, Fig. 3-7 indicated that the MWCNT content in the epoxy matrix increased as a function of the normalized thickness along the direction of the centrifugation force. This confirmed the existence of a gradient in the samples.

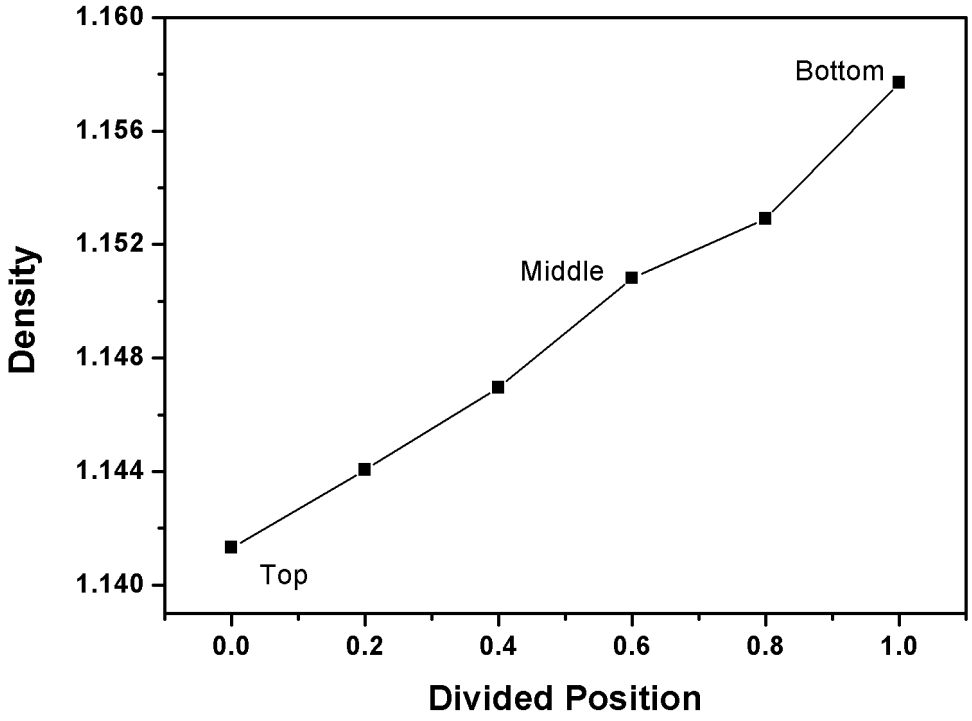

Fig. 3-7. Density of each FGM slide along the thickness direction.

3.3.3. Mechanical Behavior

For some technical applications, it would be highly desirable to have different properties at different cross-sectional positions in a material, something that is not possible using traditional composites. For example, the existence of a relatively high elastic modulus or wear resistance on the outside of a material while the inside retained normal performance could decrease unnecessary costs. An additional advantage of such materials would be the lack of any sudden changes in their properties like those present in hard coatings. These sudden changes are undesirable because they can cause stress singularities at the interface; these are associated with local failures in coatings due to spalling effects. The creation of a gradient in the filler distribution is therefore quite an effective way of solving these problems [29-30]. MWCNTs are expected to perform as excellent reinforcement fillers in functional graded composites [12-13].

The wear resistance of polymers is closely related to their viscoelastic properties [31-32], and the elastic modulus is considered to be a suitable parameter to predict wear resistance, which has a significant influence on the wear behavior [33]. The viscoelastic properties of the polymer matrix were characterized in this study. Fig.3-8 displays the storage modulus and viscous dissipation as a function of temperature, in the range 0–120°C. The storage modulus decreased abruptly (Fig. 3-8a) around the glass transition temperature (Tg, at approximately 86°C), because the FGMs had become soft. To confirm the gradient formed in the composite, the top, middle, and bottom slides of the composite were selected to be studied. The storage modulus increased gradually with increasing MWCNT content in the whole range. As shown in Fig. 3-8a, in the range of 0 to 60°C, the difference between the storage moduli of

the top and bottom samples was approximately 1Gpa. These results suggested that the gradient in the storage modulus was caused by the gradient in the MWCNT content. From Fig. 3-8b, it was clear that the value of tan delta increased with MWCNT content and that Tg also increased with MWCNT content, which further confirmed the gradient in the properties of the materials.

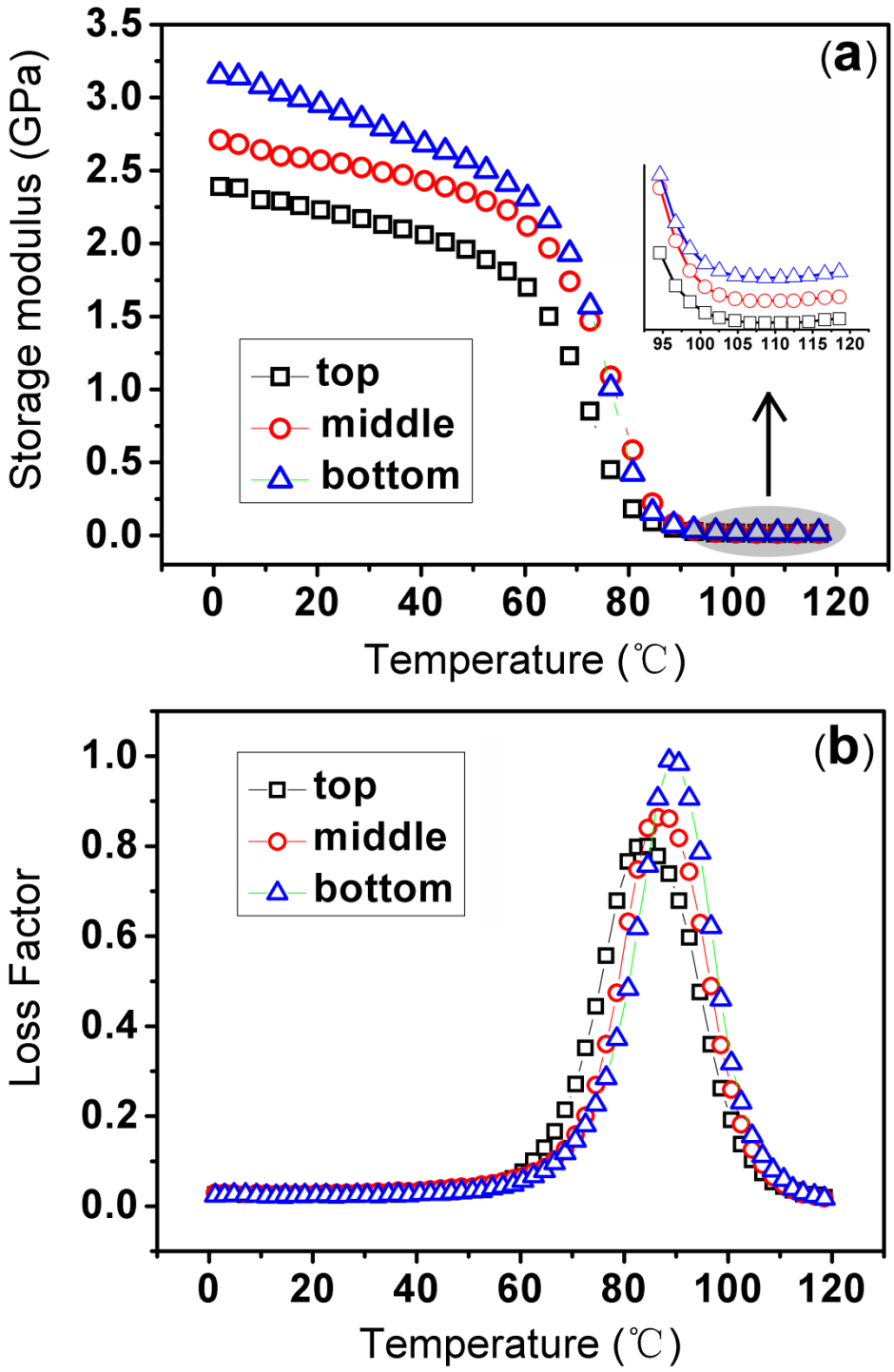

Fig. 3-8.Temperature dependence of (a) the storage modulus, and (b) the loss factor of FGM slide along the thickness direction.

3.3.4. Electrical Properties

The in-situ measured volume resistance (Fig. 3-9) exhibited an in-depth graded distribution in the matrix. Position 0.0 on the FGMs showed a volume resistance value of nearly $10^{14}\Omega\cdot$cm along the normalized thickness. This value gradually decreased to $10^{9}\Omega\cdot$cm at the middle position of 0.4, then suddenly became $10^{3}\Omega\cdot$cm at the position of 0.6, turning to a conductive state. The volume resistivity decreased drastically when the MWCNT content in the composites reached a certain level, this was due to the formation of conductive pathways in the nanocomposites over the percolation threshold. Because the electrical conductivity of the FGM followed the grading direction, this material would be ideal for applications demanding an electrically conductive surface and an insulating core.

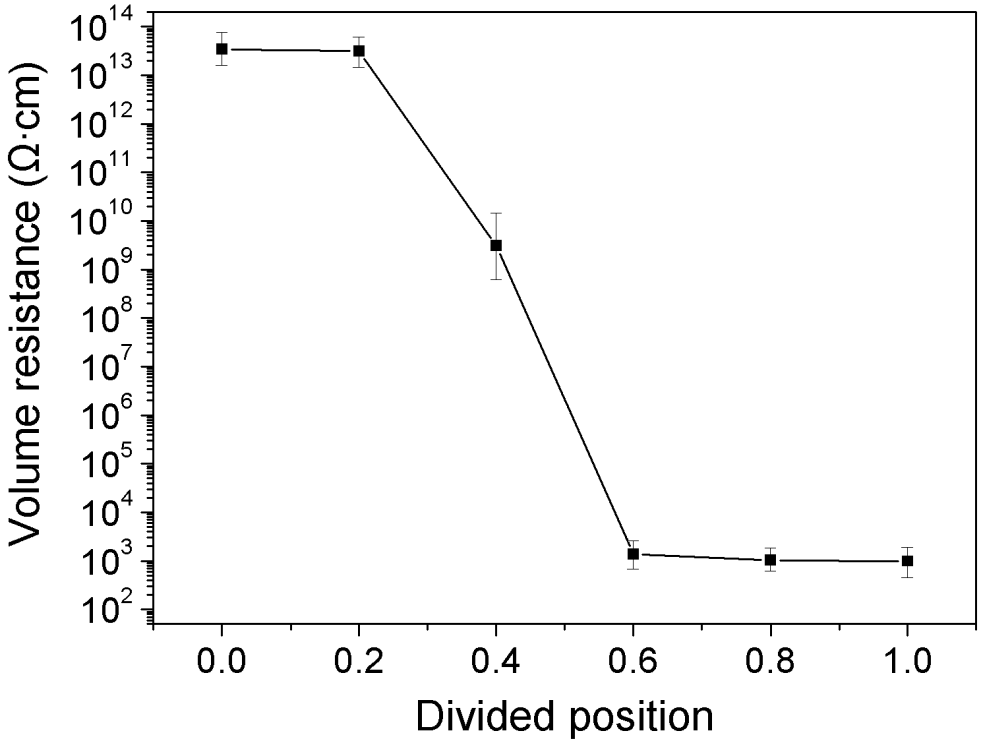

Fig. 3-9.Electrical properties of each FGM slide along the thickness direction.

3.3.5. Microwave Absorption Properties

A graded structure is considered to be a good option when designing a good microwave absorbing material [34], so the microwave absorption properties of the FGMs were investigated in this work. Fig. 3-10 shows the real and imaginary parts of the complex permittivity of the FGMs compared with those of the pure epoxy. As shown in Fig. 3-10, both the real part and imaginary part of the permittivity of the samples increases with MWCNT content from top to bottom. The real part of the permittivity was less sensitive to MWCNT content between 8 and 10 GHz except for the bottom side sample. It was also found that the permittivity was critically dependent on the frequency and decreased in inverse proportion to the frequency.

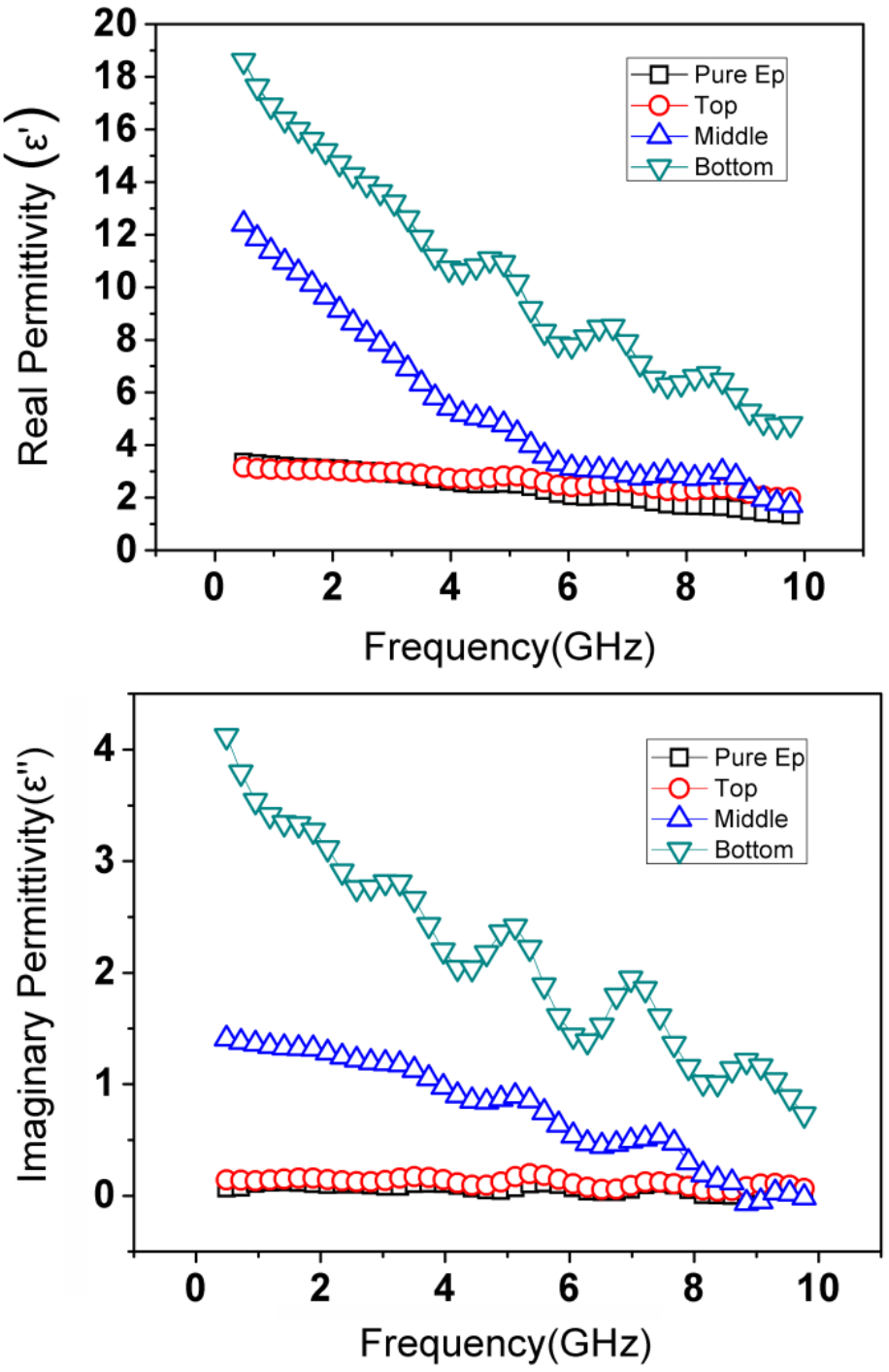

Fig. 3-10. Real part and imaginary part of permittivity of the FGMs and pure epoxy.

The dielectric loss factor and the magnetic loss factor of the bottom sample were calculated to study the intrinsic reasons for the microwave absorption of the FGMs. The results in Fig. 3-11 show the frequency dependence of the loss tangent of dielectric/magnetic of FGMs. It is obvious that the value of dielectric loss was much higher than that of magnetic loss, which suggests that the enhanced microwave absorption of the FGMs was mainly due to dielectric loss rather than magnetic loss.

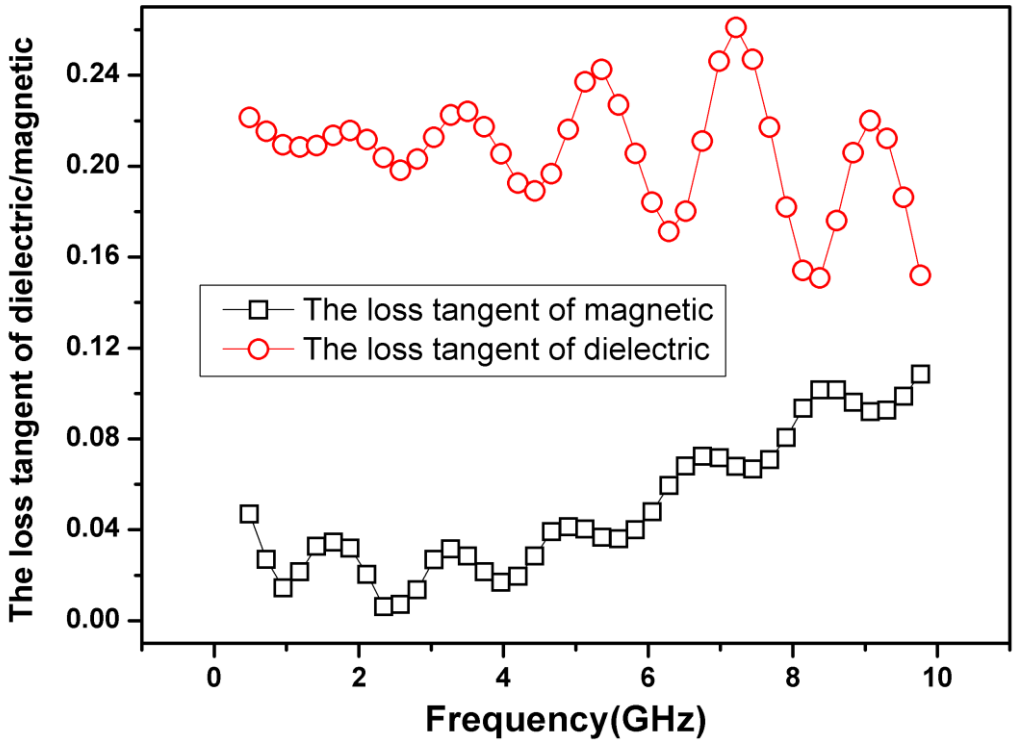

Fig. 3-11. Frequency dependency of loss tangent of dielectric/magnetic of bottom side of FGMs.

According to transmission line theory,35 we calculated the reflection loss (R.L.) of a FGMs sample with thickness of 2 mm in the range 0.5–10 GHz using the following equation:

$$\mathbf{R.L.} = \mathbf{20}\log\left|\frac{Z_{in}-1}{Z_{in}+1}\right|, \qquad (1)$$

whereZin is the normalized input impedance of a metal-backed microwave absorbing layer.

$$Z_{in} = \sqrt{\frac{\mu_r}{\varepsilon_r}}\tan h\left[j\left(\frac{2\pi fd}{c}\right)\sqrt{\mu_r\varepsilon_r}\right], \qquad (2)$$

where f is the microwave frequency in Hz, d is the thickness of the absorber in m, and c is the velocity of light in free space in m/s.

The results shown in Fig. 3-12 indicate that microwave absorption varies with MWCNT content in the FGM sample. Nam et al. (2011) reported reflection loss of -3.56 dB was measured using the composites fabricated with the thickness of 1.6 mm and 5 wt% of MWNT.37 Whereas in this work, at the position of 1.0, about 2 wt%, exhibits the best microwave absorption, and the minimum reflection loss of the bottom sample is about –3.7 dB at 10 GHz when d = 2 mm. It is obvious that a change in MWCNT content change in dielectric after the grading process affected the microwave absorption behavior.

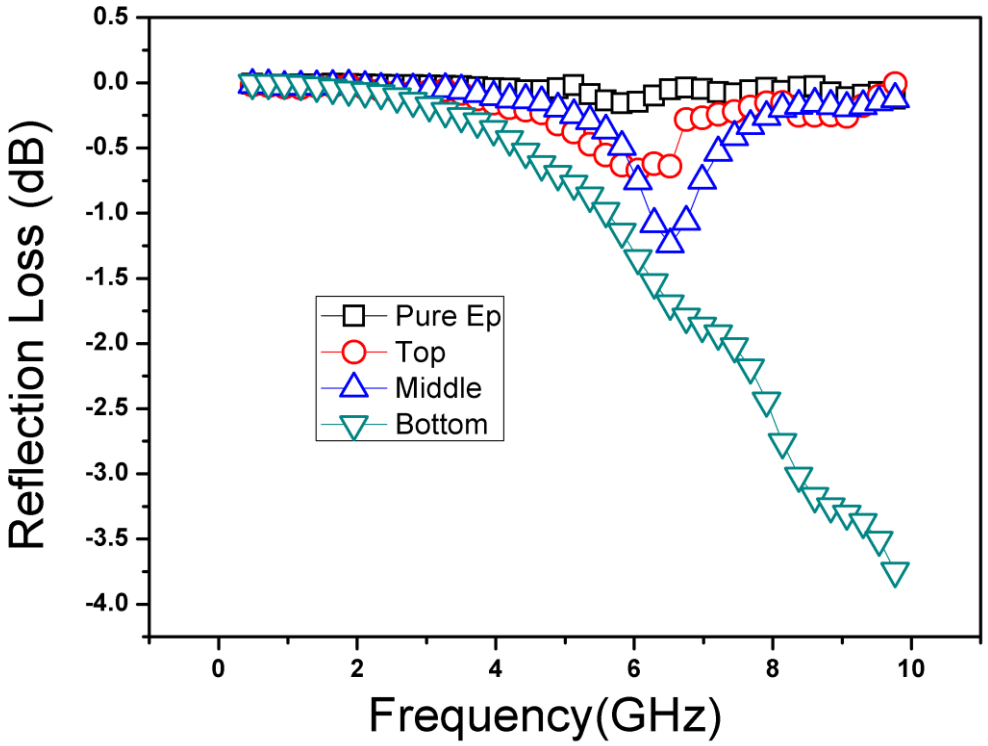

Fig. 3-12. Reflection loss curves for FGMs and pure epoxy of 2 mm thickness in the frequency range 0.5–10 GHz.

Because the reflectance of the FGMs decreases from the bottom to the top of the FGMs, according to the relation Eq. (3), microwaves can penetrate deeper into the graded structure FGMs and are thus absorbed by the MWCNTs to a greater extent than in uniformly structured materials.

$$\text{R. L.} = 10\log(1 - R). \qquad (3)$$

The shielding effectiveness (SE) results (Fig. 13) also prove the graded reflectance effect. Taking the frequency of 6.5 GHz as an example, the SE of reflection (SE_R) can be calculated according to the relation Eq. (4).36 The value of SE_R increased from top to bottom, where the top value was about 0.0 dB, the middle value about 1.3 dB, and the bottom was about 1.9 dB.

$$SE = SE_R + SE_A, \qquad (4)$$

where SE is mainly dominated by reflection (SE_R) and absorption (SE_A).

Based on the above analysis, although the absorption properties did not perform well within the range 7–10 GHz, the graded structure of the MWCNTs composites is still suggested to be a better design for microwave absorbing material in the special frequency range.

From another point of view, the graded SE in Fig. 13 shows that the bottom of the FGM reached about 6 dB at 10 GHz, which indicates that the grading method may be applicable to the fabrication of microwave shielding materials. This is because grading is an effective way to achieve high filler concentrations to enhance the SE of materials.

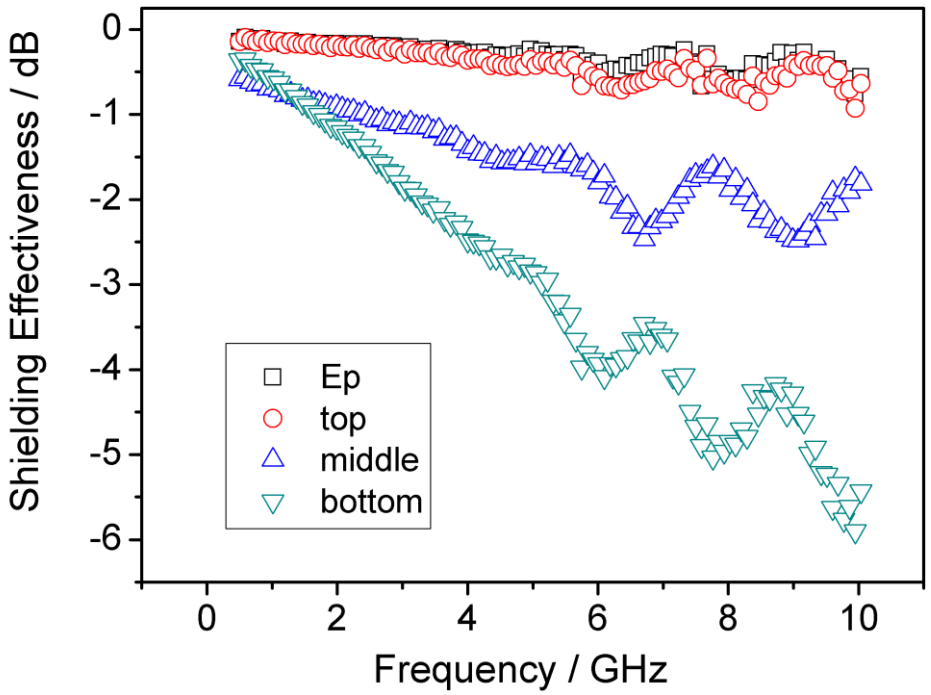

Fig. 3-13. Shielding effectiveness curves for FGMs and pure epoxy of2 mm thickness in the frequency range 0.5–10 GHz.

3.4. Summary

In brief, we successfully modified the surface of MWCNTs, and produced s-MWCNT polymer-based FGMs using a centrifugal method. The gradual incorporation of the s-MWCNTs in the epoxy resin resulted in the formation of deep-penetrating gradients in the distribution, mechanical properties, electrical properties, and microwave shielding properties. The promising grading capabilities of the s-MWCNTs indicated that it is possible to tailor the gradient of nanofillers by carefully modifying their surfaces, thus enabling grading of the properties and microstructure of the final composite material using a simple centrifugal method. The present results strongly suggest that treated nanomaterials should be considered as novel, high-performance filler candidates for the design and preparation of graded functionalities and properties compared with those used in conventional polymer composites. The FGM concept also has the potential to allow the successful, seamless joining of conventional polymer composites with polymer nanocomposites containing a high concentration of MWCNTs using the centrifugal method. These improved, nanostructure-controlled, MWCNT-containing FGMs are promising for a variety of new and challenging structural, electronic, and biomaterial applications, and may open further avenues for exploration and research.

References

1. G. N. Praveen and J. N. Reddy, Int. J. Solids. Struct., 35 (1998)4457.

2. M. Koizumi and M. Niino, MRS. Bull., 20 (1995)19.

3. F. Erdogan, Compos. Eng., 5 (1995)753.

4. C. T. Loy, K. Y. Lam and, J. N. Reddy, Int. J. Mech. Sci., 41 (1999)309.

5. Y. A. Chekanov and J. A. Pojman, J. Appl. Polym. Sci.,78 (2000)2398.

6. X.-M. Xie, Y. Chen, Z.-M. Zhang, A. Tanioka, M. Matsuoka and K. Takemura, Macromolecules., 32 (1999) 4424.

7. M. Ivosevic, R. Knight, S. R. Kalidindi, G. R. Palmese and J. K. Sutter, J. Therm. Spray. Techn., 14 (2005) 45.

8. B. Kieback, A. Neubrand and H. Riedel, Mat.Sci. Eng. A-Struct. 362, 81 (2003).

9. B. Y. Wen, G. Wu and J. Yu, Polymer., 45 (2004)3359.

10. C. Klingshirn, M. Krumova, F. Haupert and K. Friedrich, Compos. Sci. Technol.,61 (2001)557.

11. V. Parameswaran and A. Shukla, J. Mater. Sci., 33 (1998)3303.

12. H. Kwon, C. R. Bradbury and M. Leparoux, Adv. Eng. Mater.,13 (2011)325.

13. M. Estili, K. Takagi and A. Kawasaki, Scripta. Mater., 59 (2008) 703.

14. J. A. Kim, D. G. Seong, T. J. Kang and J. R. Youn, Carbon, 44 (2006) 1898.

15. Y. Watanabe, N. Yamanaka and N. Fukui, Compos. PartA., 29A (1998) 595.

16. R. Rodiguez-Castro and M. H. Kelestemur, J. Mater. Sci., 37 (2002) 1813.

17. S. S. Ray and M. Okamoto, Prog. Polym. Sci., 28 (2003) 1539.

18. P. C. Ma, J. K. Kim and B. Z. Tang,Compos. Sci. Technol., 67 (2007) 2965.

19. A. M. Shanmugharaj, J. H. Bae, K. Y. Lee, W. H. Noh, S. H. Lee and S. H. Ryu, Compos. Sci. Technol., 67 (2007) 1813.

20. X. Z. Xu, A. J. Uddin, K. Aoki, Y. Gotoh, T. Saito andM. Yumura, Carbon, 48 (2010) 1977.

21. E. B. Barros,A. G. Souza Filho, V. Lemos, J. Mendes Filho, S. B. Fagan, M. H. Herbst, J. M. Rosolen, C. A. Luengo and J. G. Huber, Carbon, 43 (2005)2495.

22. X. H. Li, Z. Cao, Z. J. Zhang and H. X. Dang, Appl. Sur. Sci., 252(22) (2006)7856.

23. Y. H. Chen, A. Lin and F. X. Gan, Appl. Sur. Sci., 252 (2006)8635.

24. E. Ukaji, T. Furusawa, M. Sato, N. Suzuki, Appl. Sur. Sci., 254(2) (2007) 563.

25. Y. Liu, W. Wongwiriyapan, K. C. Park, H. Muramatsu, K. Takeuchi, Y. A. Kim and M. Endo, Carbon, 47 (2009) 2528.

26. R. Graupner, J. Raman.Spectrosc., 38 (2007) 673.

27. H. M. Heise, R. Kuckuk, A. K. Ojha, A. Srivastava, V. Srivastavad and B. P. Asthanac,J.RamanSpectrosc., 40 (2009)344.

28. F. Tuinstra and J. L. Koenig, J. Phys. Chem., 53 (1970)1126.

29. C. Klingshirn, M. Koizumi, F. Haupert, H. Giertzsch and K. Friedrich, J. Mater. Sci. Lett., 19 (2000) 263.

30. C. Choe, C. Klingshirn and K. Friedrich, Macromol Res., 10(4) (2002)236.

31. T. L. Oberle, J. Metals., 3 (1951) 438.

32. C. Rebholz, A. Leyland, J. M. Schneider, A. A. Voevodin and A. Matthews, Surf. Coat. Technol., 120-121 (1999) 412.

33. A. Leyland and A. Matthews, Wear, 246 (2000)1.

34. M. Chen, Y. Zhu, Y. Pan, H. Kou, H. Xu and J. Guo, Mater. Design., 32 (2011)3013.

35. S. S. Kim, S. B. Jo, K. I. Gueon, K. K. Choi, J. M. Kim, K. S. Churn, IEEE

Trans.Magn., 27 (1991)5462.

36. Z. Liu, G. Bai, Y. Huang, Y. Ma, F. Du, F. Li, T. Guo and Y. Chen, Carbon, 45 (2007)821.

37. I. W. Nam, H. K. Lee and J. H. Jang, Comos. Part .A-Appl. S., 42 (2011) 1110.

38. M. Lavorgna, V. Romeo, A. Martone, M. Zarrelli, M. Giordano, G. G. Buonocore, M. Z. Qu, G. X. Fei and H. S. Xia, Eur. Polym. J., 49 (2013) 428.

39. A. Nistal, C. Palencia, M. A. Mazo, F. Rubio, J. Rubio and J. L. Oteo, Carbon, 49 (2011)1635.

40. J. H. Lee, K. Y. Rhee and S. J. Park, J. Nanosci. Nanotechno., 11 (2011) 275.

Chapter 4

Fabrication of Functionally Graded Nano-TiO_2-Reinforced Epoxy Matrix Composites under Relative Low Viscosity Environment

Fabrication of Functionally Graded Nano-TiO_2-Reinforced Epoxy Matrix Composites under Relative Low Viscosity Environment

4.1 Introduction

The concept of functionally graded materials (FGMs) was proposed in Japan in 1984, and has attracted great interest worldwide in terms of designing and combining entirely different materials to control the structure and composition in order to obtain materials with continuously changing properties and functions, for use in challenging applications [1–3]. An important area of FGM research is the development of polymer-based FGMs, which has developed rapidly because these materials are low cost, erosion resistant, and light [4–6]. Many achievements have been made in recent years. For instance, SiC particles and carbon fibers have been used as reinforcing agents in polymer matrixes, and, based on these studies, simulations of polymer-based FGMs have been developed [7, 8]. Nanoscale fillers, compared with the corresponding traditional bulk fillers, give higher-performance materials with improved properties, because of their high surface areas [9]. To achieve excellent properties and multifunctions, the introduction of grading agents such as carbon nanotubes (CNTs) is considered to be necessary [10, 11]. The use of nano-TiO_2 as a reinforcement filler gives tribological materials with excellent properties [12, 13], for the microwave absorbing material, PAni/HCl/TiO_2nanocomposite fabricated byusing TiO_2 as a filler showed a large dielectric constant [14].Phang et al. reported a novel hexanoic acid (HA) doped PAnimicro/nanocomposite containing TiO_2 and Fe_3O_4

which achieved excellent performance of microwave absorption[15]. Also, the gradient design for preparing microwave absorbing materials has been reported by Chen et al. showed impressive absorbing performance [16]. On the other hand, compared with those FGMs using CNTs, their spherical shape makes it easy to simulate the movement of nano-TiO_2 particles under centrifugation. For this reason, nano-TiO_2 is a satisfactory candidate as a reinforcing material for fabricating high-quality FGMs.

However, to date, very few research has been performed on the fabrication of nano-filler-reinforced FGMs. Kwon et al. have designed gradient layers for the fabrication of CNT-reinforced aluminum matrix FGMs using a powder metallurgy route. Estili et al. have reported CNT gradient layers in ceramic matrix composite materials fabricated using a spark plasma sintering process [10, 11]. Nevertheless, most investigations of nano-filler-reinforced FGMs have been based on numerical calculations or models. This is mainly because of the lack of appropriate processing technologies for the synthesis of composites with nano-agents from a homogenous to a graded state. Furthermore, the nano-filler can be a problem if it is hard to disperse, and in terms of interface compatibility.

In this study, we attempted to fabricate FGMs, using a centrifugal method, by controlling the parameters of centrifugation speed, centrifugation time, and viscosity [17, 18]. Epoxy resin has been used as the matrix because of its excellent mechanical properties and electrical insulation, lightness, and low cost [19]. In particular, when combined with nano-TiO_2 in bulk TiO_2–epoxy FGMs, high surface wear resistance, without interface problems, compared with coated materials, can be obtained. Unfortunately, filler aggregation occurred during fabrication, which prevented

preparation of FGMs. In this work, we focused on solving the aggregation problem, to produce high-quality FGMs, and aimed to improve the fabrication of nano-filler-reinforced FGMs.

4.2 Experimental

4.2.1 Materials and Preparation

An epoxy resin (DENATITE XNR 6815, JER 827, Nagase Chemtex Co., Ltd.) and a curing agent (DENATITE XNH 6815, Nagase Chemtex Co., Ltd.) in a weight ratio of 100:27 were used. The density was about 1.14 g/cm^3, and the viscosity under room temperature is 260 mPa·s. As the grading agent, nano-TiO_2 (density: 4.7 g/cm^3, diameter: about 50 nm; Sigma-Aldrich Co. LLC) was used. To disperse the filler uniformly, nano-TiO_2 was first pre-dispersed in the epoxy resin by sonication for 30 min at 55 °C, followed by mechanical stirring at an ultrahigh rotation speed of 18 000 rpm for 10 min and de-aeration for 15 min. A material with a TiO_2 concentration of 1 wt% was obtained. Here, we considered the viscosity to be the constant parameter; the experiments were conducted at room temperature. The optimum parameter of centrifugation for preparing the FGM is under 2000 rpm and 60 minutes, after the centrifugation process, samples were then cured and cut. The sample slices were obtained by cutting perpendicular to the direction of the centrifugal force, and were used for investigation of the FGM properties. The process is shown in Fig. 4-1(a).

Fig. 4-1(b) shows aggregation of the nano-TiO_2, which appeared at the center of the slice. To solve this problem, silanization of nano-$TiO_2$is considered an effective and solid way [20, 21]. We introduced a silane coupling agent (Z-6020, Dow Corning Toray Co., Ltd.) to modify the TiO_2 surface with the aim of improving the dispersion

in the epoxy resin and strengthening the mechanical properties of the FGMs.

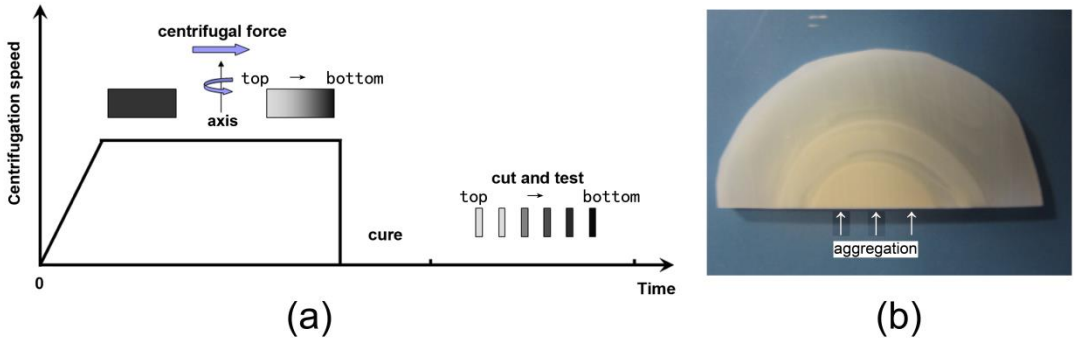

Fig. 4-1.(a) Schematic diagram of preparation of FGM samples and (b) aggregation of nano-TiO_2.

The mechanism of the silanization of TiO_2 is shown in Fig. 4-2. Prior to application of the agent, 5 vol% pure water in ethanol was prepared, and then the silane coupling agent was diluted in the water/ethanol system to give a 1 wt% solution. The amounts of coupling agent (%) added were based on the weight percentage of the filler. Prior to treatment of the TiO_2, the ethanol solution was magnetically stirred in a beaker, and the silane was added slowly to ensure uniform mixing. TiO_2 was then added slowly and the mixture was stirred continuously for 5 min for further mixing, followed by reaction for 2 h under sonication. The treated TiO_2 was then dried at 100 ℃ for 5 h to allow complete evaporation of ethanol. The treated TiO_2 (s-$TiO_{2)}$ was used to prepare the FGMs by the centrifugal method, as described above.

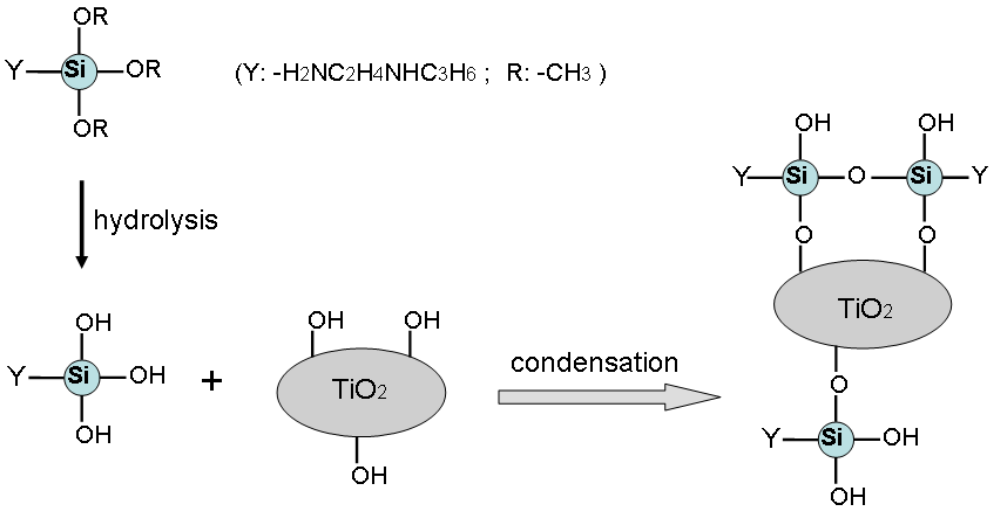

Fig. 4-2. Mechanism of silanization of nano-TiO_2.

4.2.2 Characterization

First, the densities of the slices were determined (SMK-301, Shimadzu, AW/AX/AY series). Pristine TiO_2 and s-TiO_2 were observed by transmission electron microscopy (TEM) using a JEM-2010 electron microscope with an accelerating voltage of 200 kV. X-ray photoelectron spectroscopy (XPS) analyses were performed using a Kratos Axis Ultra DLD X-ray photoelectron spectrometer with a standard Mg Kα (1256.6 eV) X-ray source, operated at 10 mA and 15 kV. All binding energies were referenced to Au (4f7/2) at 84 eV. Fourier-transform infrared (FTIR) spectra were recorded with a Shimadzu Irprestige-21 spectrometer in the region 400–4000 cm^{-1} using the KBr method. Dynamic mechanical analysis was performed at a frequency of 10 Hz in tensile mode at a 0.5% constant strain using a DVA-225 instrument (ITK, Japan). The temperature range was 0–120 ℃, with a heating rate of 2 ℃/min. The sample dimensions were 20 × 4 × 1 mm^3 (length × width × thickness). The hardness of the NR/VGCF film was measured at 10 different locations for each sample, according to ISO 868 standard, with a HARDMATIC HH337 device (Type D, Mitutoyo, Japan). The mean value was used as the hardness. The samples used for measurement of microwave absorption properties is made into a toroidal shape with an outer diameter of 7 mm, inner diameter of 3.0 mm and a thickness of 2 mm. The complex permittivity and permeability of the compound samples were measured using a vector network analyzer (37247D Anritsu Co., Ltd.) over a range of 0.5–10 GHz, and the reflection loss was calculated from the measured complex permittivity and permeability.

4.3 Results and Discussion

4.3.1 TEM analysis of s-TiO_2

The structures and morphologies of the obtained products were investigated by TEM. Fig. 4-3 shows representative TEM images of the products. Pristine TiO_2 of diameter 20–30 nm had a crystalline surface. Although the s-TiO_2 had been washed several times and sonicated in ethanol before the TEM measurements, a thin layer of thickness several nanometers was still attached to the surface of the TiO_2. It was apparent that the silane coupling agent had been successfully grafted onto the TiO_2 surface, and the grafted layer was amorphous.

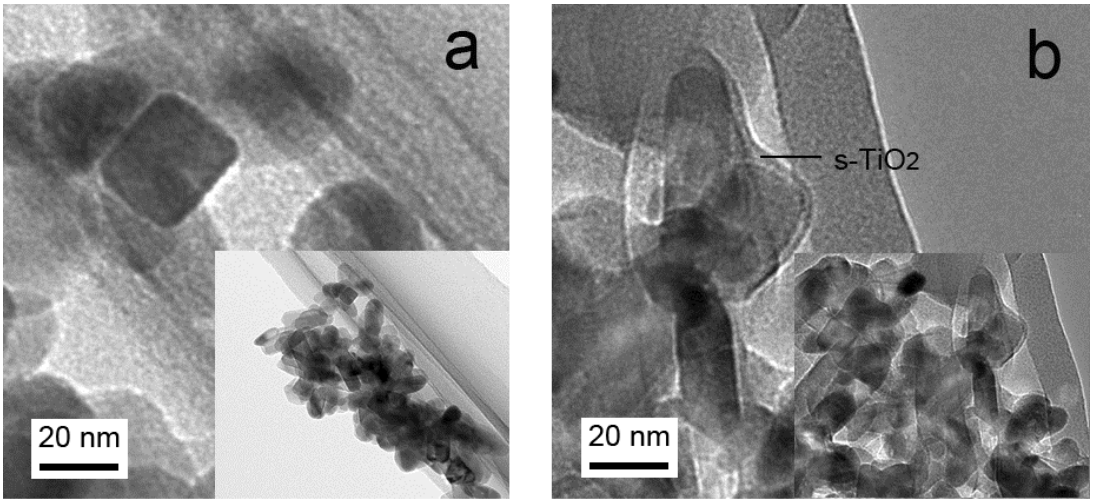

Fig.4-3. TEM images of pristine TiO_2 and s-TiO_2.

4.3.2 XPS analysis of s-TiO_2

To determine the elements in the treated TiO_2, XPS was conducted (Fig. 4-4). A typical survey spectrum of the treated TiO_2 is presented in Fig. 4-4. The survey scans of the treated TiO_2 showed the presence of Ti, O, C, N, and Si, indicating that the TiO_2 surface was silanized. For comparison with s-TiO_2, a survey scan of pristine TiO_2 was also conducted; in the typical survey spectrum, the peak from C cannot be avoided because of the poor adhesion of the TiO_2 to the tape when preparing the XPS sample.

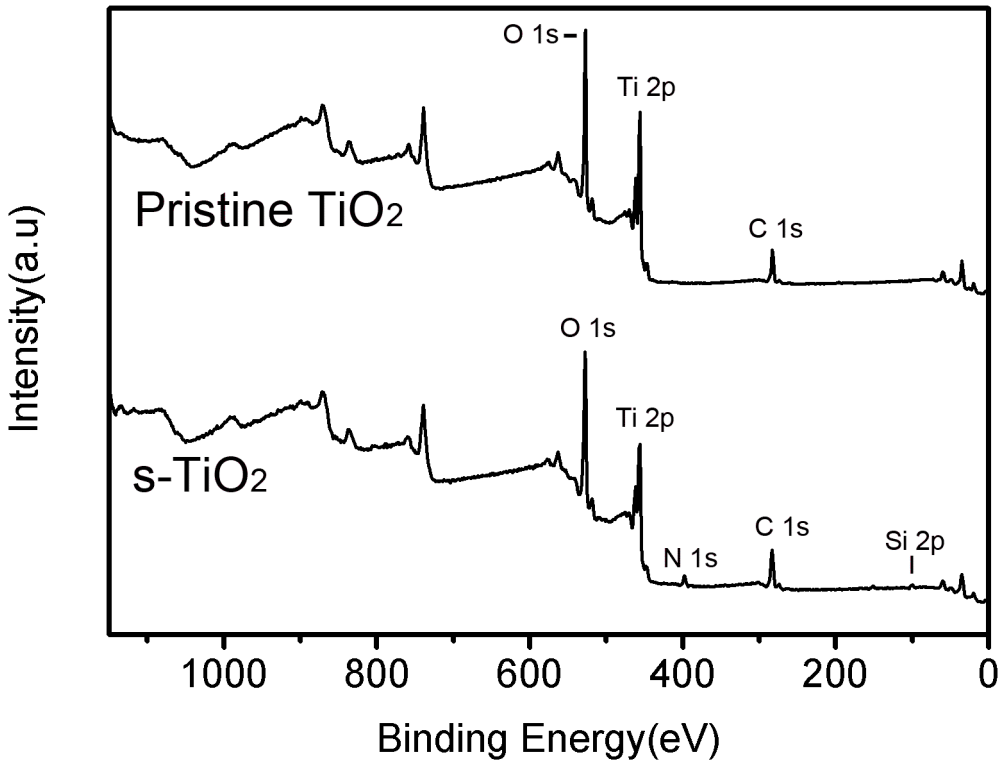

Fig. 4-4. XPS spectra of pristine TiO_2 and s-TiO_2.

4.3.3 FT-IR analysis of s-TiO_2

Fig. 4-5 shows the FTIR spectra of TiO_2 and s-TiO_2. Fig. 4-5(a) shows the spectrum of pristine TiO_2, which is featureless, whereas the spectrum of s-TiO_2 (Fig. 4-5b) has abundant peaks because of the grafted silane layer. The wide peak from 900 cm^{-1} to 400 cm^{-1} was assigned to the Ti–O vibration [22]. The peaks located at 1041 cm^{-1} and 1137 cm^{-1} were attributed to the Si–O–Si stretching vibration [23], indicating that a dehydration polycondensation reaction occurred between the silane coupling agents. The peak at 1360 cm^{-1} corresponded to the stretching vibration of C–H [24], and the peaks at 2933 cm^{-1}, 2883 cm^{-1}, and 1455 cm^{-1} resulted from C–H vibrations [25]. The peaks at 1664 cm^{-1} and 1590 cm^{-1} were assigned to the deformation vibration of NH_2 [23]. The peak at 3370 cm^{-1} was connected with the stretching vibration of O–H, which formed on the TiO_2 surface as a result of water adsorption. These results indicate that grafting of functional groups onto nano-TiO_2 can be achieved by silanization, making it possible to improve the TiO_2 dispersion in epoxy resin.

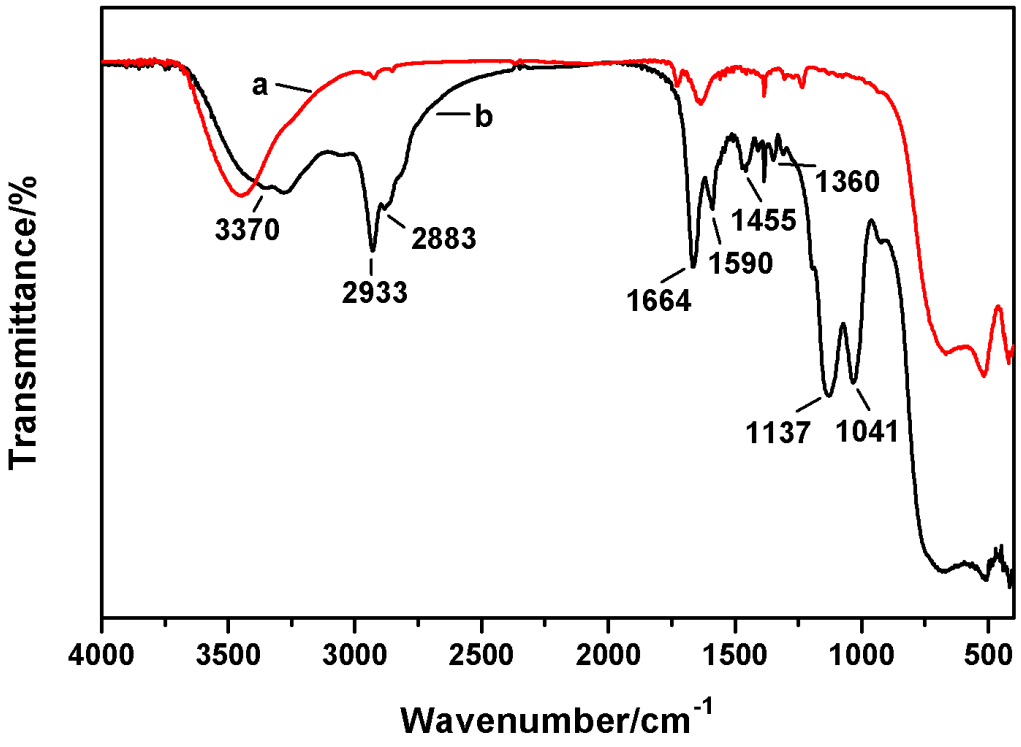

Fig. 4-5. FTIR spectra of (a) pristine TiO_2 and (b) s-TiO_2.

4.3.4 TiO_2 Distribution

We considered that the aggregation occurred in the epoxy-curing stage, before the TiO_2 silanization, because the viscosity became very low when the temperature was increased. The nanoparticles will aggregate more easily than when the viscosity is high. Fig. 4-6 shows the density of each FGM slice after treatment of the nano-TiO_2. The results indicate that the content of TiO_2 in the epoxy substrate increased as a function of the normalized thickness along the centrifugal force direction, which confirmed a gradient.

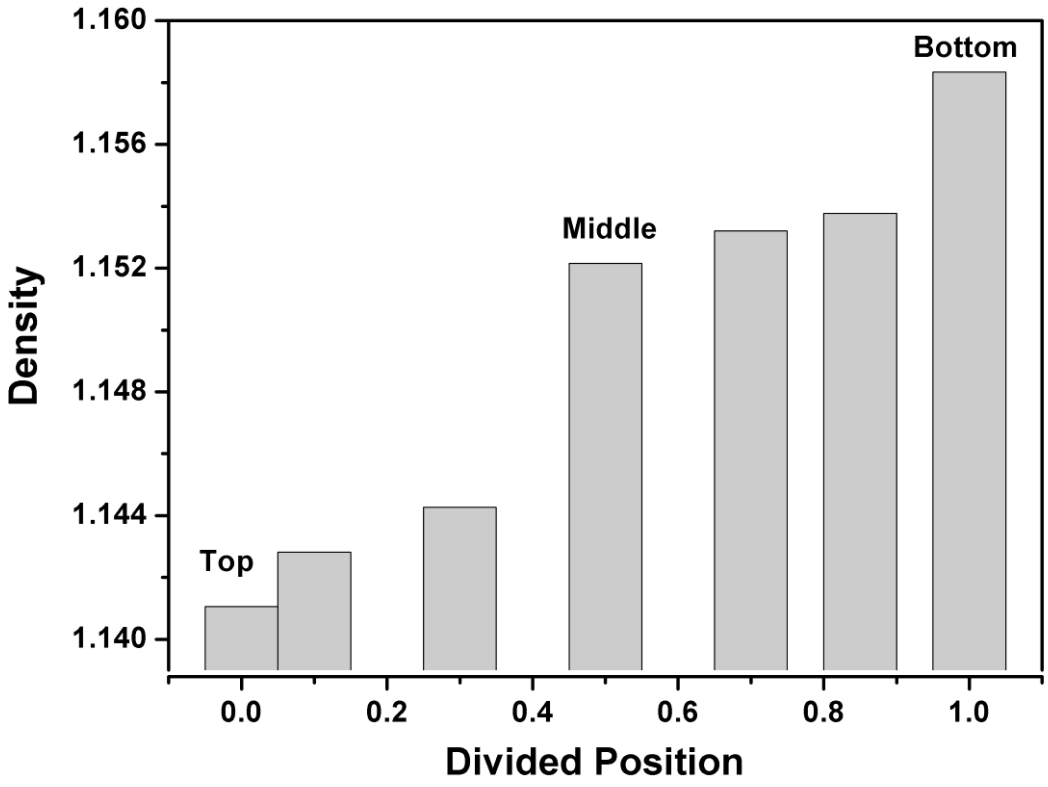

Fig. 4-6.Density of each slice of FGM along the thickness.

4.3.5 Mechanical Properties

There are some technical applications, such as in gears, in which it is useful to have different properties at different locations in the cross-section of the component. This could be a higher hardness and wear resistance on the outside and a higher toughness and damage tolerance at the inside. Also, sudden property jumps, for example, in hard coatings, are undesirable since these can cause stress singularities at interfaces, associated with local coating failure as a result of spalling-off effects. For these purposes, the creation of a filler distribution gradient is an effective way of preparing wear-resistant materials [26, 27]. TiO_2 is very popular as a reinforcing filler for preparing wear-resistant composites [12, 13]. Hardness and elastic modulus are considered to be suitable parameters for predicting the wear resistance of materials [28]. In this study, characterization of the viscoelastic properties and hardness was carried out.

Viscoelastic Properties and Hardness

The wear resistance of polymers is closely related to their viscoelastic properties [29–31], and the elastic modulus, in particular, has a very important influence on the wear behavior. Fig.4-7 shows the storage modulus and viscous dissipation as a function of temperature from 0 °C to 120 °C. At around the glass-transition temperature (*T*g, about 86 °C), the storage modulus decreased suddenly, because the FGMs were transformed to a soft state. To confirm the gradient formed in the composite, the top, middle, and bottom slices of the composite were selected and studied. With increasing TiO_2 content, the storage modulus increased gradually in the range from 0 °C to 60 °C. As shown in the figure, the difference between the top and

the bottom is an increase of about 1 GPa. This result suggests that the gradient in the storage modulus was caused by a gradient in the TiO_2 content.

Hardness is regarded as a primary material property defining wear resistance, and was also investigated. Fig. 4-8 shows the hardness of every slice of the FGM, and the increasing tendency of the hardness along the normal is obvious. From top slice of the FGM to the bottom, the hardness increases 2.5-fold. The hardness gradient is also indirect evidence that design of a gradient of wear resistance can be achieved.

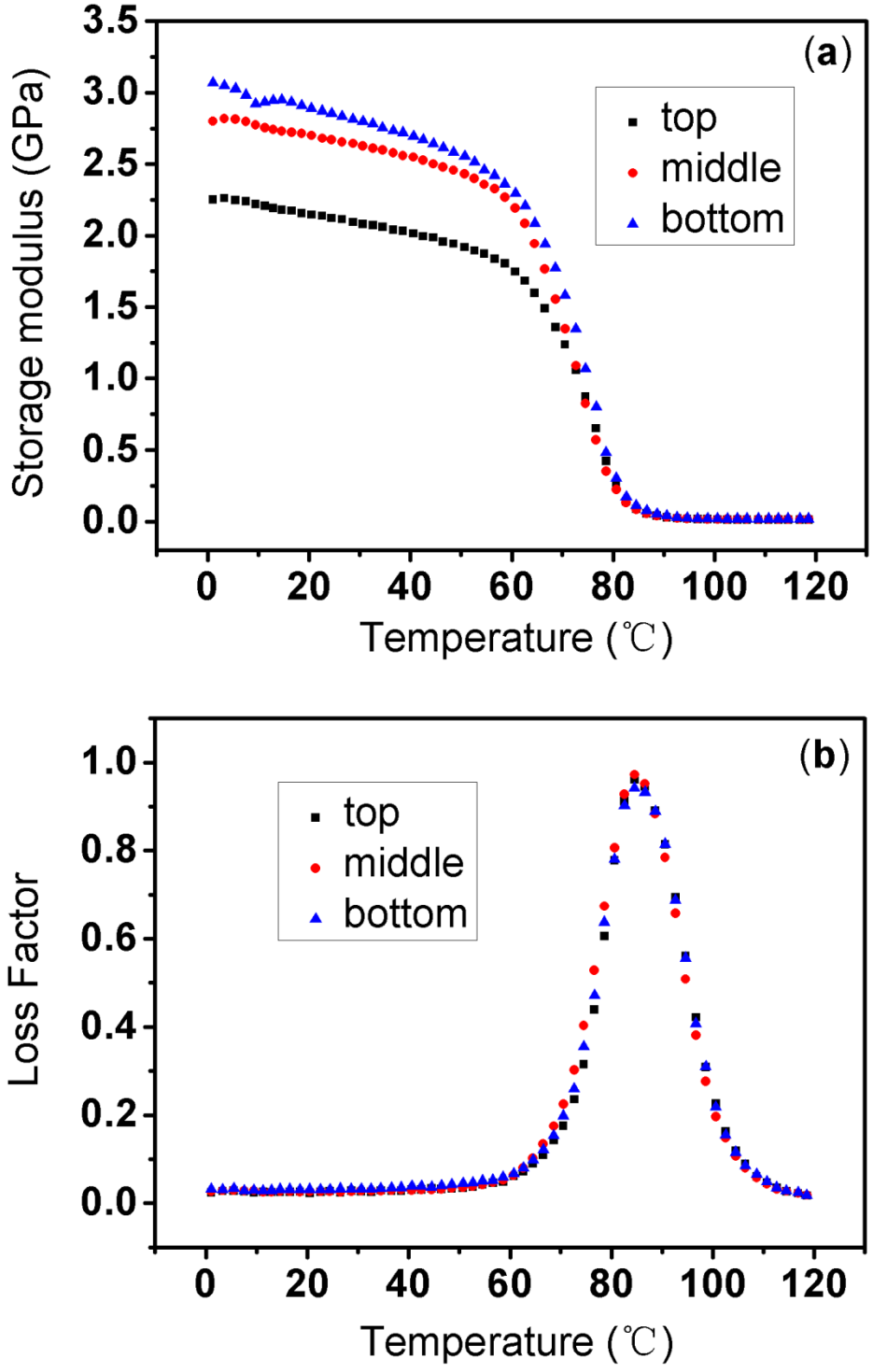

Fig. 4-7. Temperature dependence of (a) the storage modulus and (b) the loss factor of FGM slice along the thickness.

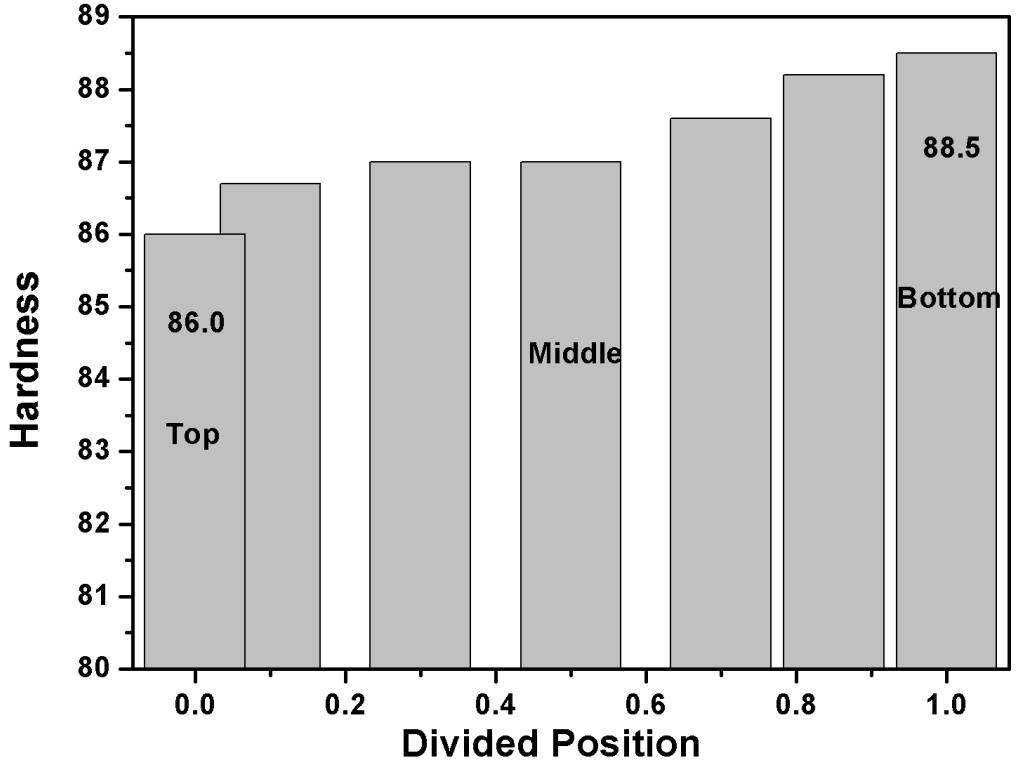

Fig. 4-8. Hardness of each slice of FGM along the thickness.

4.3.6Microwave absorption properties

Microwave absorbing ability of the uniform structure material can be improved through the gradient structure design, because the gradient absorbing properties lead to a greater absorbing ability for the entire material [16]. Thus we investigated the absorption properties of the FGMs.

Firstly, the real and imaginary parts of the complex permittivity ($\varepsilon^{*}=\varepsilon'-j\varepsilon''$) of the FGMs and the pure epoxy were measured. As shown in Fig. 4-9, compared to pure epoxy and the top slice, the bottom and the middle slices of FGMs shows relative high value of the real part and imaginary part of the permittivity in the range of 0.5-10GHz. It is also found that the permittivity is critically dependent on the frequency and decreases in inverse proportion to the frequency.

The loss tangent of dielectric can be calculated by using the formula $\tan\delta = \varepsilon''/\varepsilon'$, which could be used to predict the absorbance of nanocomposites [32]. It is considered that higher $\tan\delta$ indicates stronger absorption. The results in Fig. 4-10 shows frequency dependence of the loss tangent of dielectric of FGMs. It is found that the value of the bottom and the middle slices are relative higher in the high frequency from 8 to 10 GHz compared with pure epoxy and top slice. It is also found that three main peaks appeared at around 5, 7, and 9 GHz which can predict that stronger microwave absorption can be obtained in the these area.

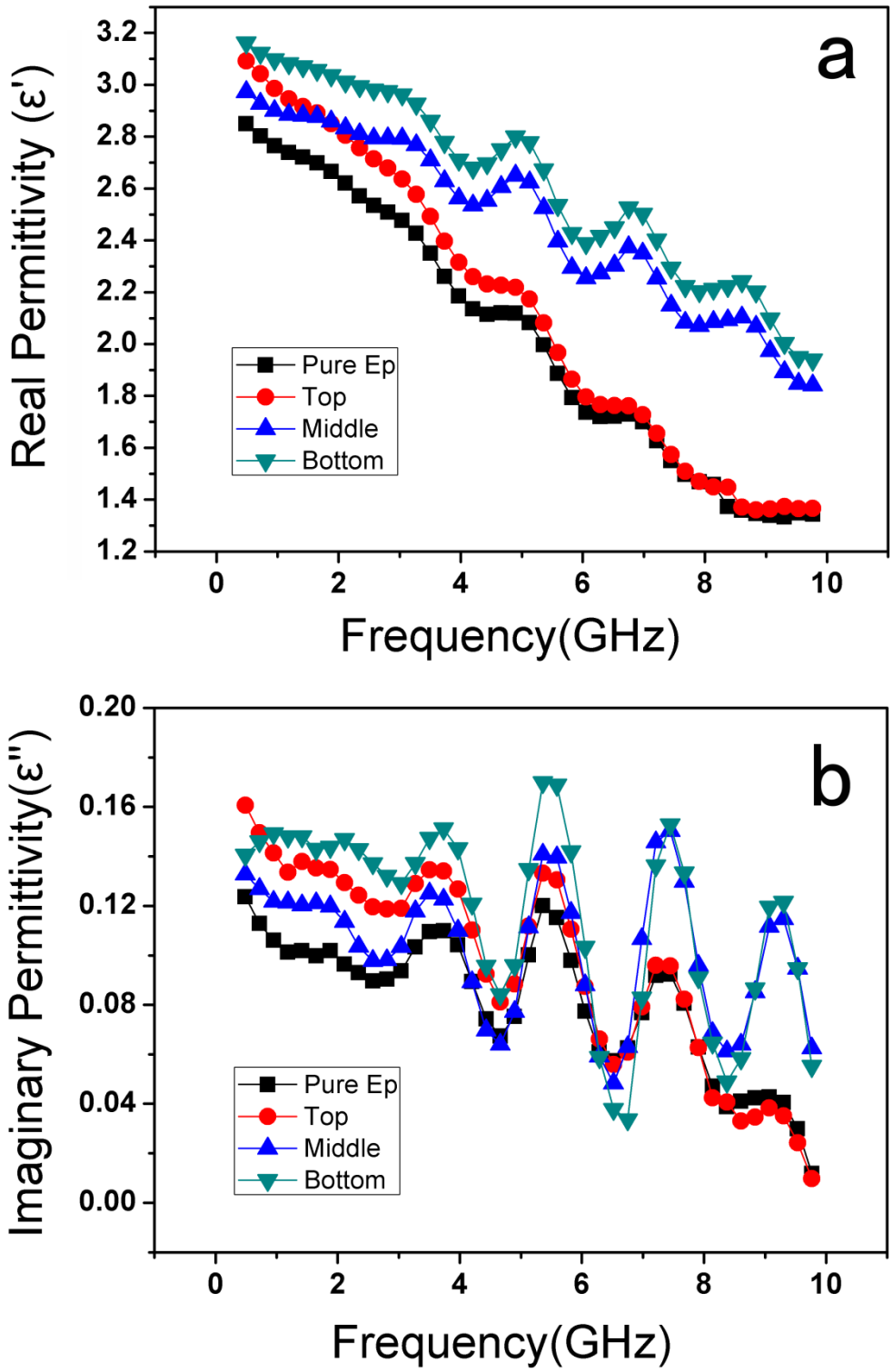

Fig. 4-9. Real part (a) and imaginary part (b) of permittivity of FGMs and pure epoxy.

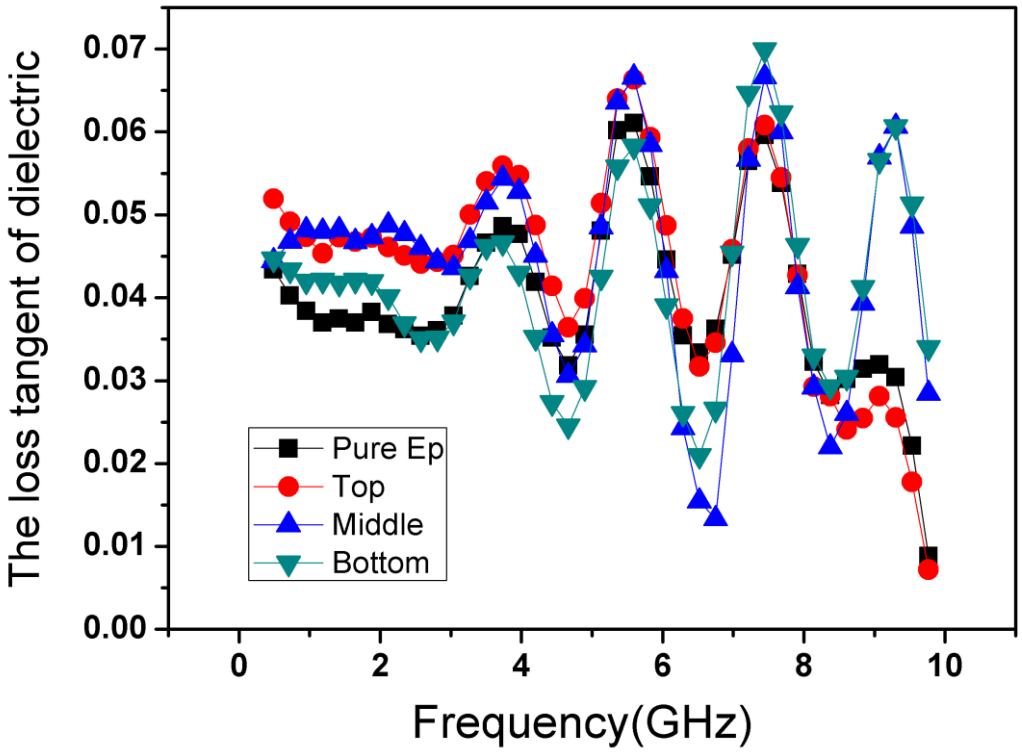

Fig. 4-10. Frequency dependency of loss tangent of dielectric of pure epoxy and FGMs.

The reflection loss (R.L.) of the FGMs sample with thickness of 2mm in 0.5-10 GHz was calculated. as shown in Fig. 4-11, according to transmission line theory [33], as:

$$R.L. = 20 \log \left| \frac{Z_{in}-1}{Z_{in}+1} \right| (1)$$

Z_{in} is the normalized input impedance of a metal-backed microwave absorbing layer.

$$Z_{in} = \sqrt{\frac{\mu_r}{\varepsilon_r}} \tanh \left[j \left(\frac{2\pi f d}{c} \right) \sqrt{\mu_r \varepsilon_r} \right] (2)$$

where f is the microwave frequency in Hz, d is the thickness of the absorber in m, and c is the velocity of light in free space in m/s.

In general, high conductivity, dielectric permittivity, and magnetic permeability of the materials contribute to high microwave absorption [34]. Due to low concentration of the TiO_2 and insulation, good absorbing properties cannot be achieved, however, absorption properties act in good agreement with the prediction. It also shows the graded microwave absorption to a certain degree, but the top slice shows relative higher value at the peak around 6.5 GHz, this may due to the size effect of nano-TiO_2 [15], because in the centrifugation process, the spherical filler size gets bigger, the movement of the filler gets faster, in this situation, the smaller size of nano-TiO_2 remained in the top slice performed relative high absorption.

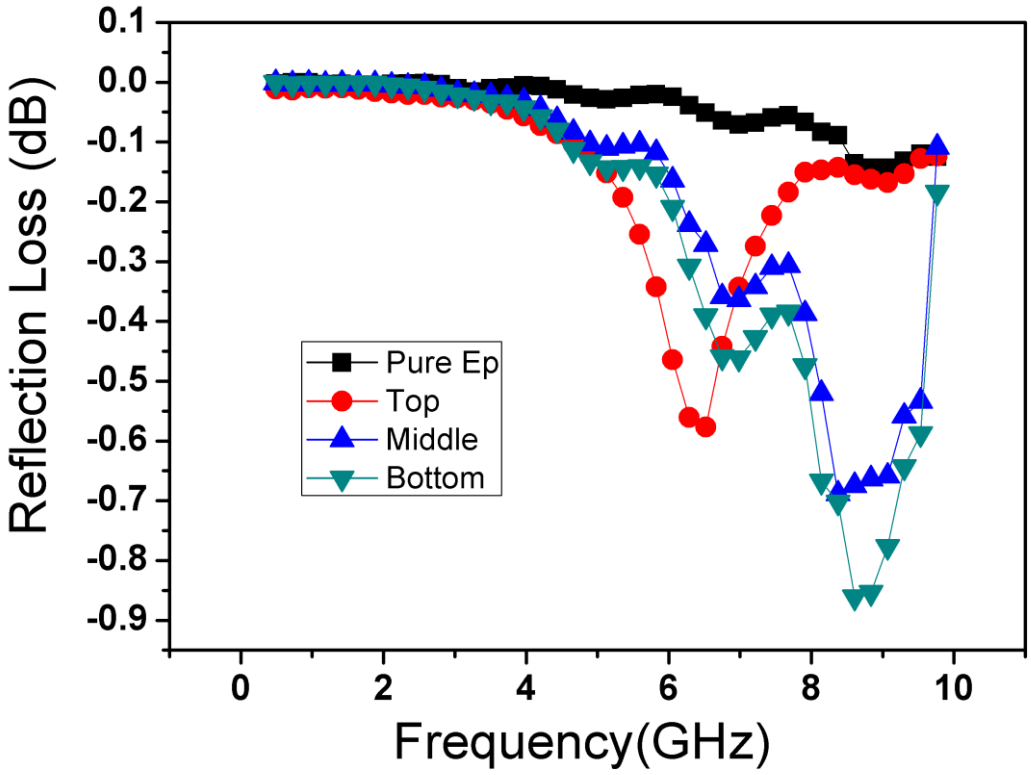

Fig. 4-11. Reflection loss curves for FGMs and pure epoxy with 2 mm thickness in the frequency range of 0.5-10 GHz.

4.4 Summary

The aggregation problem of TiO_2 have been successfully resolved by modification with silane agent, and confirmed by the result of TEM images, XPS investigation and FTIR test. Also we successfully produced s-TiO_2-incorporated polymer-based FGMs using a centrifugal method. The gradual incorporation of s-TiO_2 into the epoxy resin effectively caused depth gradients in the s-TiO_2 distribution, mechanical properties and dielectric property of the composite. The gradient of the hardness and storage modulus of slices of FGMs may suggest that wear resistance materials can be designed in the gradient structure, and thus reduce the filler consumption in the unnecessary area which lead to a lower cost. The loss tangent results predicted the microwave absorption behavior, and the absorption properties also shows the gradient performance to a certain degree. The promising s-TiO_2 grading capability indicated that it is possible to tailor desired gradient nanofiller composites.

References

1. M. Koizumi and M. Niino, MRS. Bull., 20(1995)19.

2. Y. Watanabe, Y. Inaguma, H. Sato and E. Miura-Fujiwara, Mater., 2(2009) 2510.

3. Y. Watanabe, H. Sato and T. Ogawa, Mater. Trans., 48(2007) 2945.

4. C. Klingshirn and M. Koizumi,J. Mater. Sci. Lett., 19(2000)263.

5. S.A.R. Hashmi and U.K. Dwivedi, Polym. Eng. Sci., 46(2006)1660.

6. N. Chand and A.M. Naik, Polym. Compos.,29(7) (2008) 736.

7. T. P. D. Rajan, R. M. Pillai and B. C. Pai, Mater. Charact.,61(2010) 923.

8. L. Drenchev, J. Sobczak, and S. Malinov. Model. Simul. Mater. SC., 11(2003) 651.

9. D. R. Paul and L. M. Robeson, Polym., 49(2008) 3187.

10. H. Kwon, C. R. Bradbury and M. Leparoux, Adv. Eng. Mater., 13(2011) 325.

11. M. Estili, K. Takagi, and A. Kawasaki, Scripta. Mater., 59(2008) 703.

12. N. Dejang, A. Watcharapasorn, and S. Wirojupatump, Surf. Coat. Tech., 204(2010) 1651.

13. L. Chang, Z. Zhang and C. Breidt, Wear., 258(2005) 141.

14. A. Dey, S. De, A. De, and S.K. De, Nanotechnology., 15(2004) 1277.

15. S.W. Phang, M. Tadokoro, J. Watanabe, N. Kuramoto, Polym. Adv. Technol.6 (2009) 550.

16. M.Chen, Y.Zhu, Y.Pan, H.Kou, H. Xu, and J.Guo, Mater. Design.,32 (2011) 3013.

17.Y.Watanabe, N.Yamanaka and N.Fukui, Compos. PartA, 29A(1998)595.

18. R. Rodiguez-Castro and M.H. Kelestemur, J. Mater. Sci., 37(2002)1813.

19. SS. Ray and M. Okamoto, Prog. Polym. Sci., 28(2003) 1539.

20. J. Lin, J.A. Siddiqui and R.M. Ottenbrite, Polym. Advan. Technol., 12 (2001)285.

21.M. Sabzi, S.M. Mirabedini, J. Zohuriaan-Mehr and M. Atai, Prog. Org. Coat., 65 (2009) 222.

22. H. Wellmann, J. Rathousky and M. Wark, Micropor. Mesopor. Mat., 44(2001) 419.

23. E. Ukaji, T. Furusawa, M. Sato and N. Suzuki, Appl. Surf. Sci., 254(2007) 563.

24. X.H. Li, Z. Cao, Z.J. Zhang, and H.X. Dang, Appl. Surf. Sci., 252(2006) 7856.

25. Y. H. Chen, A. Lin and F. X. Gan, Appl. Surf. Sci., 252(2006) 8635.

26. Siddhartha, P. Amar and D.B. Amba, Mater. Design., 32 (2011) 615.

27. K. Friedrich, Z. Zhang and A.K. Schlarb, Compos. Sci. Technol., 65x (2005) 615

28. A. Leyland and A. Matthews, Wear, 246 (2000) 1.

29. W. Brostow, and H.E. HaggLobland, Polym. Eng. Sci., 48 (2008) 1982.

30. H.X. Jiang, Q.Q. Ni, and T. Natsuki, Polym. Compos.,32 (2011)675.

31. W. Brostow, H.E. HaggLobland, and M. Narkis, J. Mater. Res., 21 (2006) 2422.

32. A.M. Darren, H. Trisha, Synth. Met., 156 (2006) 497.

33. S.S. Kim, S.B.Jo, K.I. Gueon, K.K. Choi, J.M. Kim, and K.S. Churn, IEEE Trans.Magn., 27(1991)5462.

34. C.Y. Lee, H.G. Song, K.S. Jang, E.J. Oh, A.J. Epstein, and J. Joo, Synth. Met., 102 (1999) 1346.

Chapter 5

Theoretical Analysis of EMI SE by Absorption between FGM and Homogeneous Material

5.1 Introduction

Nowadays, the electromagnetic interference (EMI) have become a serious problem because of the high speed development of electrical device [1-2]. Not only the electromagnetic (EM) wave will affect the normal function of the electronic equipments, but also it will influence human health. Surround by the EM wave, an appropriate microwave absorber is highly needed to control the excessive self-emission of electromagnetic waves and also defend the external electromagnetic wave. Microwave absorbers are also very important in military and aerospace industries, application like coating the absorbers on the surfaces of military equipment helps to avoid detection by the radar [3-4]. But the disadvantages of the coating material cannot be ignored such as low adhesion, low environment adaptation and poor mechanical properties. Novel absorbing material with high performance of both absorbing ability and strong mechanical properties is highly demanded. Studies on materials with unique structure such as multilayers and foam, and preparation of polymer-based FGMs are a promising candidate for EMI absorbing materials because of its low cost, light weight, flexible and highly processable [5-8]. The FGMs can be applied in various challenging environments, for absorption properties, it can widen bandwidth by adjusting complex permittivity and permeability to satisfy the principle of impedance match. Already the relative experiments have been reported, Xiao et al. synthesized Electrically conducting polyaniline–magnetic oxide (Fe3O4) composites by emulsion polymerization in the presence of dodecyl benzene sulfonic acid as the surfactant and dopant and ammonium persulfate as the oxidant. The microwave absorption of functionally graded material (FGM) was simulated by the computer

according to the principle of impedance match and the calculated results agreed quite well with the experimentally measured data [9].

Although Xiao's material contains the magnetic oxide which can enhance the absorbing ability, but the graded structure also played an important role. In our work, we tried to give an analytical discuss on the EM absorbing properties of homogeneous material (HM) and the FGM of VGCF-based epoxy composites.

5.2 Analysis of EM absorption

The electromagnetic waves that compose electromagnetic radiation can be imagined as a self-propagating transverse oscillating wave of electric and magnetic fields. Maxwell derived a wave form of the electric and magnetic equations, thus uncovering the wave-like nature of electric and magnetic fields, and their symmetry. According to Maxwell's equations, a spatially varying electric field is always associated with a magnetic field that changes over time. Likewise, a spatially varying magnetic field is associated with specific changes over time in the electric field. In an electromagnetic wave, the changes in the electric field are always accompanied by a wave in the magnetic field in one direction, and vice versa. There are two cases that should be considered for EMI shielding, the near-field and far-field. The far-field is defined as distances further than $\lambda/2\pi$ between the radiation source and shielding material, where λ is the wavelength of the electromagnetic wave. In this work, the electromagnetic wave used to test shielding materials was limited to a plane wave in the far-field. The SE is expressed as:

$$SE = 10\log\frac{I}{T} \qquad (1)$$

Where I is the incident power, and T is the transmitted power.

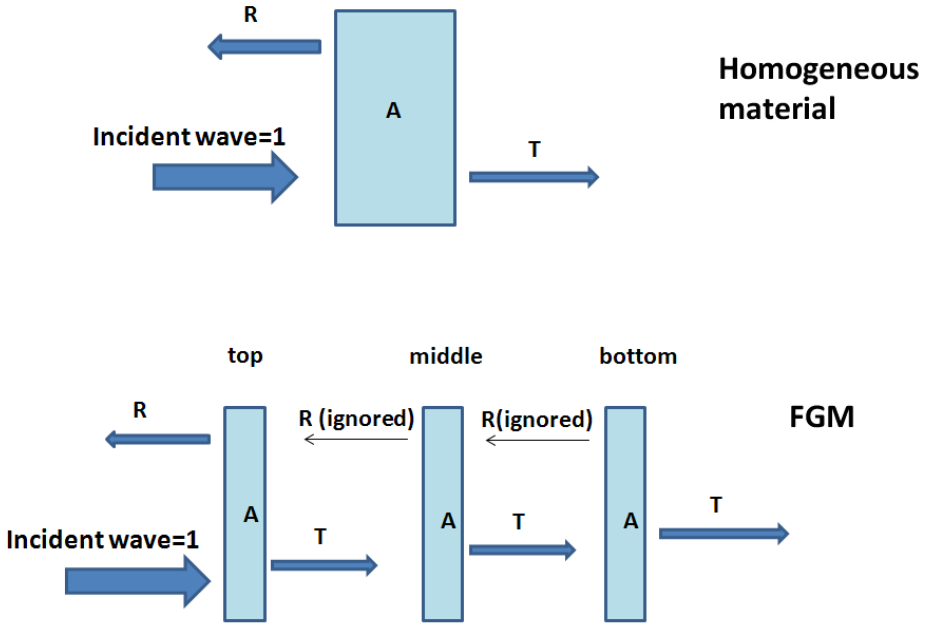

Fig 5-1 Schematic diagram of shielding in HM and FGM.

As shown in Fig 5-1, when an electromagnetic wave propagates to a shielding material, a typical process is as follows: part of the wave is reflected (R) on the surface of the material, which strongly depends on the impedance matching; part of the wave is absorbed (A), and dissipated as heat; part of the wave is multi-reflected inside the shielding material; and the others transmitted (T) through the material. Based on the description above, the electromagnetic wave shielding is mainly dominated by three functions: reflection (SE_R), absorption (SE_A), and multi-reflection (SE_M), and can be represented by equation (2):

$$SE=SE_R+SE_A+SE_M \qquad (2)$$

These three functions further relate to the intrinsic permittivity, permeability, conductivity, and thickness of the material and the frequency of the electromagnetic wave.

The skin depth (δ) is defined as the distance at which the electric field decreases to 1/e of its incident strength, which is expressed as follows:

$$\delta = 1/\sqrt{\pi f \mu \sigma} \qquad (4)$$

where f is the wave frequency, μ is the permeability, and σ is the electrical conductivity in S/m. The data we used here come from the prepared VGCF/epoxy FGMs in chapter 2 and it can be regarded as nonmagnetic, thus $\mu=\mu_0=4\times10^{-7}$H/m, where μ_0 is the permeability in free space. The multi-reflection can be ignored if the shielding material is thicker than the skin depth. Therefore, we assume the power of incident wave as 1, the equation can be described as:

$$1=A+R+T \qquad (5)$$

In this part, we tried to discuss the absorption properties. In this case, for a very special analysis, the reflection part is not concerned.

According to Al-Saleh et al. [10], for conductive materials, SE_A can be described as follows:

$$SE_A = 8.7\frac{d}{\delta} = 8.7d\sqrt{\pi f \mu \sigma} \qquad (6)$$

For a continuous graded material under ideal condition, as presented in Fig 5-1, because the interface usually existed in the HM is disappeared in FGM, therefore,

based on the perfect impedance match, the reflection can be ignored among every part of FGMs. Also because of the poor conductivity of the top part of FGMs, the reflection on the top can be ignored either.

The conductivity used in chapter 2 was expressed in Ω·cm，the calculation used here have to expressed in S/m, thus we converted the unit by the following relationship: S/cm=1/(Ω·cm)=100S/m.

Fig 5-2 presents the conductivity of FGMs along the normalized thickness.

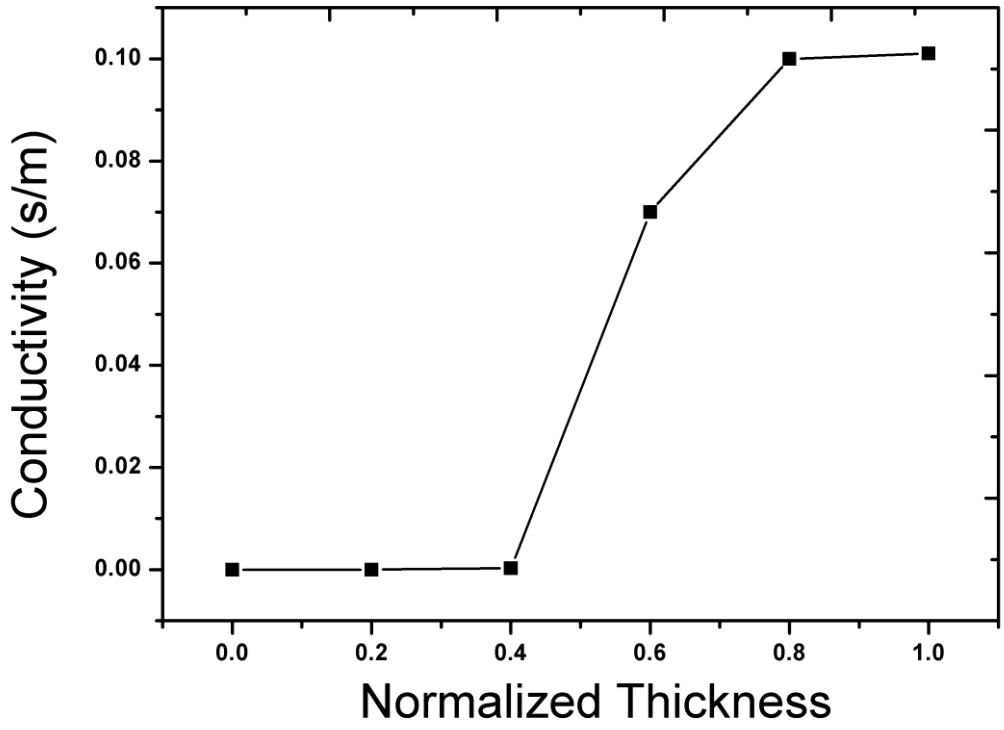

Fig 5-2 Conductivity of FMGs along the normalized thickness.

The absorption described in dB is shown in Fig 5-3, in the range of 2-10 GHz, the absorption performance of HM shows almost the same effect besides the bottom part of FGMs.

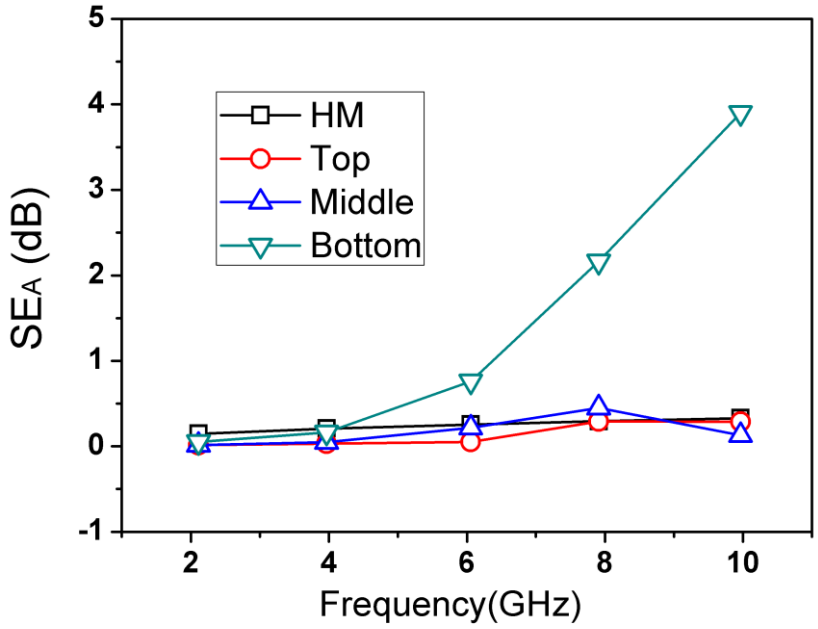

Fig 5-3 Absorption shielding effect of HM and FGM with frequency by calculation.

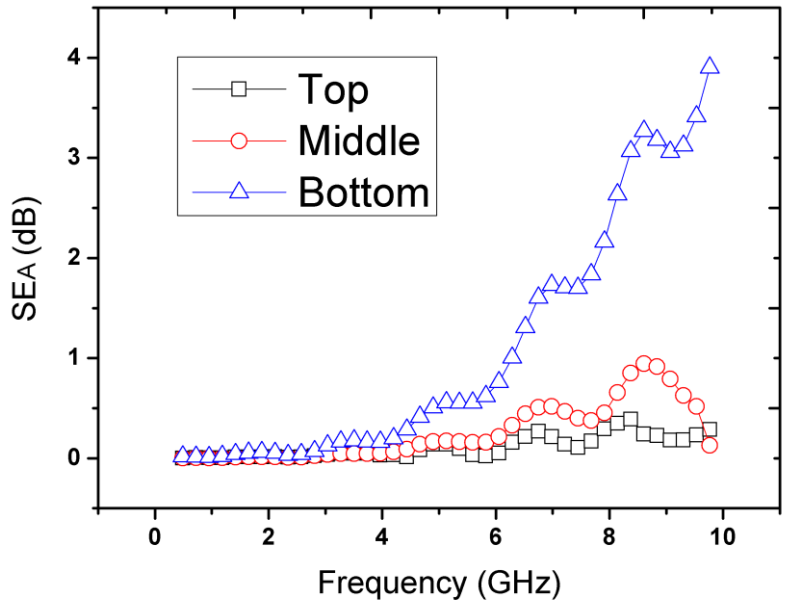

Fig 5-4 Absorption shielding effect of FGM with frequency by experiment.

In order to do a comparison between the calculation and the experiment, the tested absorption properties of FGMs was showed in Fig 5-4. Although this is not perfectly matched with calculation value, in the real environment, the peak appeared cannot be predicted by calculation, but the tendency and main value matched well. As a result, the prediction of absorption of FGMs by calculation is considered to be feasible and reasonable.

The table presents the percentage of absorption, at the low range of frequency, the absorbing ability is very weak, and it increases with the increment of frequency. The highest absorption is in the bottom part of FGM with the value of 59.3% due to the high conductivity.

Table - EMI SE by absorption

f(GHz)	HM(%)	FGM(%)		
		Top	Middle	Bottom
2	3.3	0.4	0.4	1.2
4	4.7	0.7	1.2	3.6
6	5.7	1.2	5.0	16.1
8	6.1	6.7	9.8	39.2
10	7.3	6.4	3.0	59.3

Although it is obviously that FGMs shows a better EM absorption performance. The whole absorption of FGMs is calculated and compared with that of HM in Fig5-5. As mentioned above in Fig 5-1, the incident wave power is defined as 1, as shown in the table above, the power gradually absorbed by each part along the normalized thickness of the FGMs. Thus the total percentage of the absorption can be calculated and expressed in Fig 5-5.

Generously, the absorption depends on the frequency, and increases with increment of frequency. In the low frequency region, the HM has almost the same absorption effect with FGM, but in the higher frequency region, higher than 4 GHz, the FGMs showed much higher percentage of absorption effect.

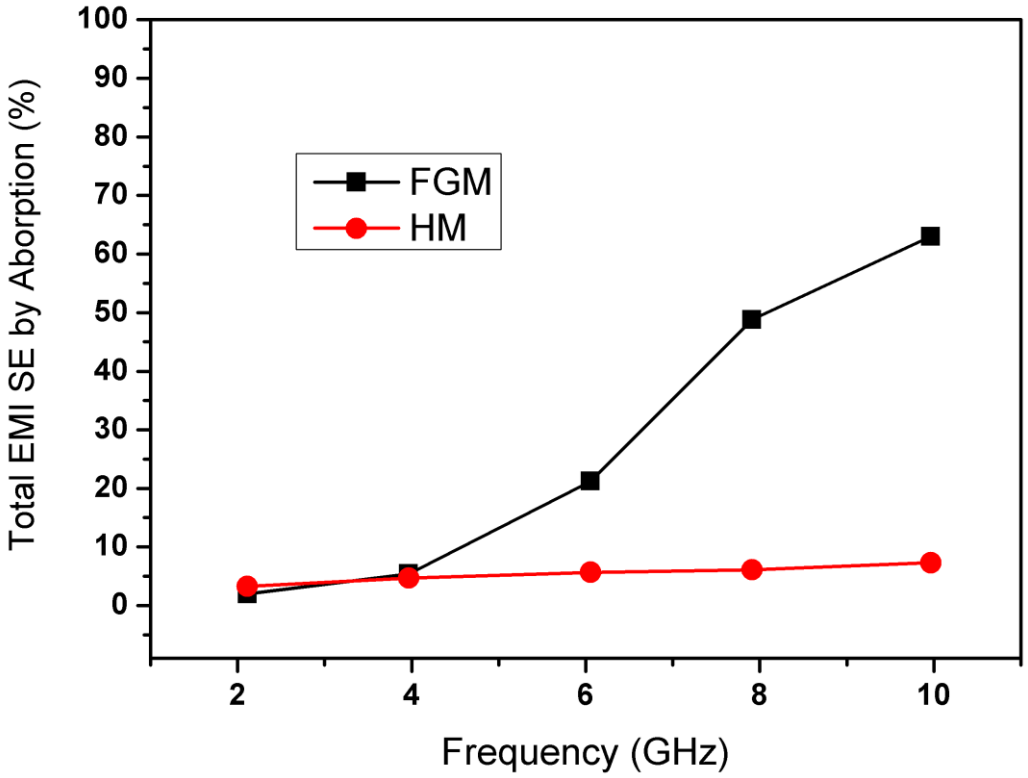

Fig 5-5 Comparison of the absorption performance between HM and FGM.

5.3 Summary

In short, the FGMs have a better absorption property than HM in the whole range of frequency. Based on the analysis above, we consider that the absorption properties of FGMs can be predicted by the calculation, in this case, prior to fabricating, the demanded absorbing ability of FGMs may designed in advance, which can be used to instruct the preparing. In this work, the graded structure design is suggested to fabricate the EM wave absorbing materials and the analytical comparison between HM and FGMs materials is discussed.

References

[1]D. D. L.Chung, Carbon, 39 (2001) 279.

[2]H. M. Kim, K. Kim, C. Y. Lee, Appl. Phys. Lett., 84 (2004) 589.

[3]S. M.Abbas, A. K.Dixit, R.Chatterjee, J.Magn.Magn. Mater.,309 (2007) 20.

[4] F. Wuyou; L.Shikai,W. Fan, J.Magn.Magn. Mater., 316 (2007) 54.

[5]Y. L. Yang, M. C. Gupta, Nano.Lett., 5 (2005) 2131.

[6] N. Dishovsky, M.Grigorova, Mater. Res. Bull., 35 (2000) 403.

[7]S. Motojima, S.Hoshiya, Y. Hishikawa, Carbon, 41 (2003) 2658.

[8]C. C. Lee, D. H. Chen, Appl. Phys. Lett., 90 (2007).

[9] X. Han,Y. S. Wang, Phys. Scr. T129 (2007) 335.

[10]M. H.Al-Saleh, U. Sundararaj,Carbon,47 (2009) 1738.

Chapter 6

General Conclusions

For developing the nanofiller employed and polymer based FGMs, this dissertation contained possible methods to fabricate the FGM which may applied in many ways. The obtained results may be remarked as follows.

In **chapter 2**, we successfully produced VGCF-incorporated polymer-based FGMs using the centrifugal method. The gradual VGCF incorporation within an epoxy resin effectively caused depth gradients in the tribological behavior, electrical conductivity and microwave absorption properties. The VGCF grading capability indicated that it is possible to tailor desired gradient distribution of filler content by careful selection of the processing parameters, thus to control precisely variations in the properties and microstructure. The FGMs fabricated in this work may be applied in some special advanced material areas. For instance, the friction coefficient gradients of the FGMs would enable the development of some technical applications, e.g., gears or rollers, in which a high sliding resistance on the outside is needed. The gradients in electrical conductivity can be considered to be ideal for applications demanding an electrically conductive surface and an insulating core for FGMs. As for the microwave absorbing material, the graded structure may be a better design.

In **chapter 3**, we modified the surface of MWCNTs, and produced s-MWCNT polymer-based FGMs using a centrifugal method. The gradual incorporation of the s-MWCNTs in the epoxy resin resulted in the formation of deep-penetrating gradients in the distribution, mechanical properties, electrical properties, and microwave shielding properties. The promising grading capabilities of the s-MWCNTs indicated that it is possible to tailor the gradient of nanofillers by carefully modifying their surfaces, thus to enable grading of the properties and microstructure of the developed nanomaterials. The present results strongly suggest that treated nanomaterials should

be considered as novel, high-performance filler candidates for the design and preparation of graded functionalities and properties compared with those used in conventional polymer composites. The FGM concept also has the potential to allow the successful, seamless joining of conventional polymer composites with polymer nanocomposites containing a high concentration of MWCNTs using the centrifugal method. These improved, nanostructure-controlled, MWCNT-containing FGMs are promising for a variety of new and challenging structural, electronic, and biomaterial applications, and may open further avenues for exploration and research.

In **chapter 4**, the aggregation problem of TiO_2have been successfully resolved by modification with silane agent, and confirmed by the result of TEM images, XPS investigation and FTIR test. Also we successfully produced s-TiO_2-incorporated polymer-based FGMs using a centrifugal method. The gradual incorporation of s-TiO_2 into the epoxy resin effectively caused depth gradients in the s-TiO_2 distribution, mechanical properties and dielectric property of the composite. The gradient of the hardness and storage modulus of slices of FGMs may suggest that wear resistance materials can be designed in the gradient structure, and thus reduce the filler consumption in the unnecessary area which lead to a lower cost. The loss tangent results predicted the microwave absorption behavior, and the absorption properties also shows the gradient performance to a certain degree.

In **chapter 5**, we discussed the EM wave absorption ability of FGMs and HM, the FGMs have a better absorption property than HM in the whole range of frequency. The graded structure design is suggested to used to fabricate the EM wave absorbing materials.

In short, nanofillers (VGCF, MWCNT, TiO2) were employed to fabricate the

epoxy based FGM using the centrifugation method, also the properties of these FGMs have been characterized, These achievements strongly suggest that nanosized materials could be employed as novel multifunctional materials for manipulating and designing multi-FGMs within conventional polymer materials. And it is promising for use in a variety of new and challenging structural, electronic, and military applications, and may open up further areas for intensive exploration and research.

Acknowledgements

I am very thankful that all the people around me gave me really great help during my study years, I cannot complete this dissertation without them.

First of all, I would like to thank my supervisor Prof. Qing-Qing Ni who gave me the opportunity to do research here and also gave me so many advice and help.

I am particularly grateful to Prof. Limin Bao, Prof. Yasushi Murakami, Prof. Toshiaki Natsuki and Prof. Jianhui Qiu for accepting to be a co-referee of this thesis.

Also, I'd like to express my gratitude to global COE of Shinshu University for financial support both on my study and my daily life.

Finally, I want to thank all my friends especially Dr. Zhu Yaofeng in the laboratory and my family.

List of Publication

[1] **Yi Wang**, Qing-Qing Ni, Yaofeng Zhu, Toshiaki Natsuki, Development of Functionally Graded Vapor-Grown Carbon-Fiber/Polymer Materials, Polymer Composites, Volume 34 Issue: 10 Pages: 1774-1781 Published: OCT 2013.

[2] **Yi Wang**, Qing-Qing Ni, Yaofeng Zhu, Toshiaki Natsuki, Functionally Graded Epoxy Composites Using Silane Coupling Agent Functionalized Multiwalled Carbon Nanotubes, Nano, Volume 09, Issue 01, Published: Jan 2014.

[3] **Yi Wang**, Qing-Qing Ni, Yaofeng Zhu, Toshiaki Natsuki, Fabrication of Functionally Graded Nano-TiO_2-Reinforced Epoxy Matrix Composites, Polymer Composites, Volume 35, Issue 3, pages: 557-563, Published: March 2014.